AD-A112 239 ROCKWELL INTERNATIONAL THOUSAND OAKS CA MICROELECTR--ETC F/G 20/6
OPTICAL COMMUNICATION FOR INTEGRATED CIRCUITS.(U)
MAR 82 P D DAPKUS N00014-80-C-0501
UNCLASSIFIED MRDC41072.1FR NL

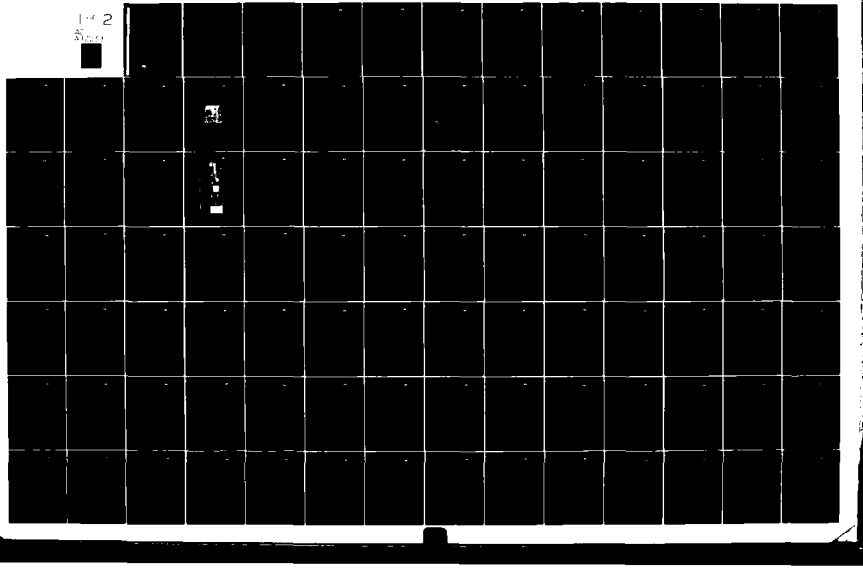

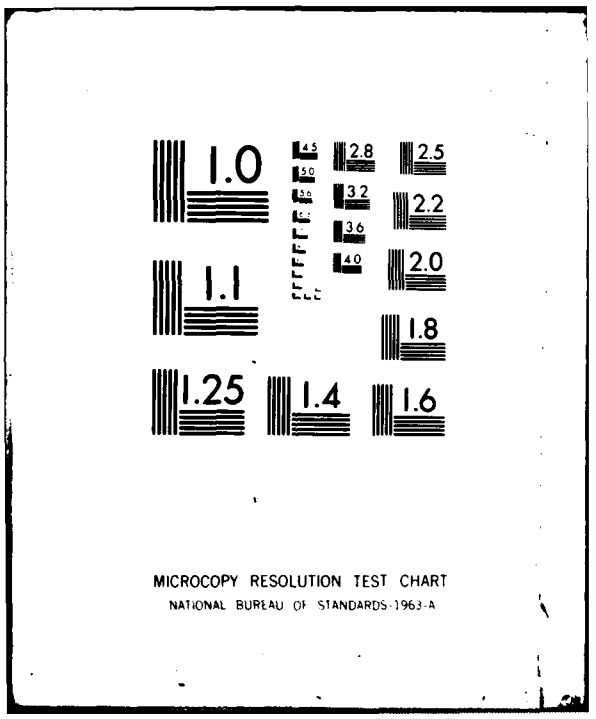
1.0
1.1
1.25
1.4
1.6
1.8
2.0
2.2
2.5
2.8
3.2
3.6
4.0
MICROCOPY RESOLUTION TEST CHART
NATIONAL BUREAU OF STANDARDS-1963-A

(12)

MRDC41072.1FR

Copy No. 1

OPTICAL COMMUNICATION FOR INTEGRATED CIRCUITS

FINAL REPORT FOR THE PERIOD
June 1, 1980 through November 15, 1980

CONTRACT NO. N00014-80-C-0501

Prepared for

Physical Sciences Division
Office of Naval Research
800 North Quincy St.
Arlington, VA 22217

P.D. Dapkus
Program Manager

MARCH 1982

Rockwell International

unclassified

SECURITY CLASSIFICATION OF THIS PAGE (When Data Entered)

REPORT DOCUMENTATION PAGE	READ INSTRUCTIONS BEFORE COMPLETING FORM
1. REPORT NUMBER	2. GOVT ACCESSION NO. AD A112239	3. RECIPIENT'S CATALOG NUMBER
4. TITLE (and Subtitle) Optical Communication for IC's	5. TYPE OF REPORT & PERIOD COVERED Final Report 06/01/80 through 11/15/80
	6. PERFORMING ORG. REPORT NUMBER MRDC41072.1FR
7. AUTHOR(s) P. D. Dapkus	8. CONTRACT OR GRANT NUMBER(s) N00014-80-C-0501
9. PERFORMING ORGANIZATION NAME AND ADDRESS Rockwell International/Microelectronics Research and Development Center, 1049 Camino Dos Rios, Thousand Oaks, CA 91360	10. PROGRAM ELEMENT, PROJECT, TASK AREA & WORK UNIT NUMBERS
11. CONTROLLING OFFICE NAME AND ADDRESS Scientific Officer, Director, Electronic & Solid Sciences Program, Physical Sciences Div., Office of Naval Research, 800 N. Quincy St., Arlington,	12. REPORT DATE March, 1982
	13. NUMBER OF PAGES
14. MONITORING AGENCY NAME & ADDRESS(if different from Controlling Office) 11. cont. VA 22217 Att: Mr. Max N. Yoder Re: Contract No. N00014-80-C-0501	15. SECURITY CLASS. (of this report)
	15a. DECLASSIFICATION/DOWNGRADING SCHEDULE

16. DISTRIBUTION STATEMENT (of this Report)

Approved for public release; distribution unlimited

17. DISTRIBUTION STATEMENT (of the abstract entered in Block 20, if different from Report)

18. SUPPLEMENTARY NOTES

19. KEY WORDS (Continue on reverse side if necessary and identify by block number)

Very high speed integrated circuit (VHSIC), microprocessor, optical transmission, optical interconnection, transmitter drive power, monolithic integration, integrated optoelectronics, fanout, broadcast transmission, state-of-the-art, generic techniques, laser technology, biconical fused taper coupler, high Q cavity, narrow diffused stripe lasers, Bragg

20. ABSTRACT (Continue on reverse side if necessary and identify by block number)

This report summarizes a study of the feasibility of interconnecting high speed GaAs integrated circuits by the transmission of optical energy. Data rates in excess of 2 Gb/s will require an interconnect technology other than hard-wire. The monolithic integration of optical devices with electronic circuitry makes high-data-rate optical data transmission possible.

This study examined the requirements on lasers, laser drivers, detectors, preamplifiers, and optical distribution networks to make data transmission between

DD FORM 1 JAN 73 1473 EDITION OF 1 NOV 65 IS OBSOLETE

unclassified

SECURITY CLASSIFICATION OF THIS PAGE (When Data Entered)

20. IC chips feasible. These requirements have led to the selection of certain device designs and optical distribution networks for use in optical interconnect. To assess the performance of an optically interconnected system, such issues as power dissipation, optical losses, and geometrical size were assessed for each configuration.

It is concluded that optical interconnection of circuits is feasible under certain circumstances. No generally applicable interconnect scheme is recommended; rather each system must be considered for its own merits and uses. Several important conclusions are reached concerning transmitter and receivers for interconnect.

(1) The geometry can be made as small as present day bonding pads.

(2) The power dissipation for optical data transmission is negligible for system size IC's.

(3) Guided wave networks must be used for interconnecting systems on a circuit board.

The technologies required for implementing interconnect are identified, and a program plan to develop these technologies is presented.

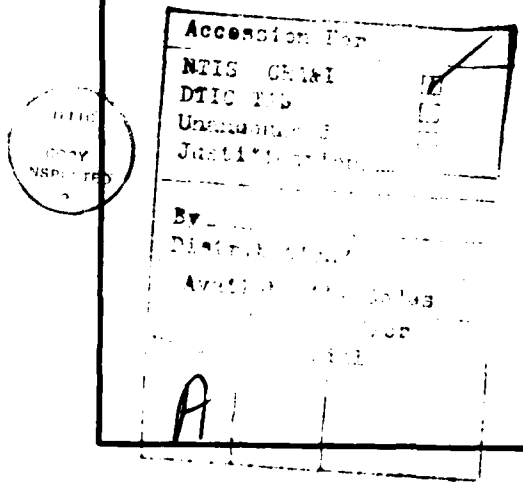

TABLE OF CONTENTS

TABLE OF CONTENTS (continued)

LIST OF FIGURES

LIST OF FIGURES

LIST OF FIGURES

1.0 INTRODUCTION

The performance of high speed high density GaAs and Si integrated circuits (IC's) is progressing at a rapid pace. Silicon IC's with over 100,000 transistors are readily available commercially. As the VHSIC (very high speed integrated circuit) program runs its course, Si IC's with pin counts in excess of 200 pin's will become commonplace.

GaAs IC's, although not as complex, are advancing in a functional throughput rate and complexity. GaAs inherently operates at higher speeds than Si, typically in the range of two to four GHz. As a result, the input and output data for these devices clock at rates in excess of two GHz. The GaAs technology has developed to the point where LSI (1000 gates) circuitry can readily be fabricated, and the trend towards VLSI circuitry is proceeding at a rapid pace. It is expected that by the end of the 1980's a GaAs microprocessor will be demonstrated.

With the rapid advancement of these two technologies, interconnection looms as a common problem that may limit the complexity and speed at which this circuitry can operate. In the case of Si IC's, the problem involves the density of the interconnects. The interconnection of subsystem chips containing 200 pins with one another by the use of standard multilayer printed circuit board will become impractical if not impossible. Alternate means must be devised to interconnect these circuits. Similarly, as the density of GaAs circuits increases to VLSI complexity, the interconnection of circuits operating in the one to four GHz range represents a limiting factor in the complexity of systems that can be assembled with existing technology.

A potential solution to these problems is the interconnection of the circuits by the use of optical transmission. The optical interconnection of integrated circuits and subsystems brings to the electronic circuit and system designer the advantages of optical communications. These include wide bandwidth, immunity from noise, improved transmission security, high sensitivity, and immunity from ground loops. In addition, because of the ultra low loss

and wide bandwidth available in optical fibers today, it is possible to interconnect circuits or subsystems operating at very high data rates separated by large distances with no transmitter drive power penalty. This is to be contrasted with an electrically interconnected system in which increased distances between circuits is accommodated by large increases in drive power.

The bandwidth of optical communication systems is approaching data rates as high as four Gb/s. This is accomplished by the monolithic integration of sources and detectors with the electronic drive circuitry and receivers and is thus sometimes called integrated optoelectronics. Based on results to be provided in this report, it appears that optical interconnect using monolithically integrated optoelectronic circuits is a reasonable way to interconnect GaAs integrated circuits operating at frequencies as high as four GHz.

This report will analyze the prospects for optically interconnecting high speed GaAs circuits. Certain assumptions concerning the mode of transmission and degree of fanout have been used in performing the analysis contained in the report. They are:

1) Data transmission will occur in packet form with the destination and originator of the data specified in the header of the data packet. This form of transmission permits both point-to-point and broadcast transmission of the data. It allows maximum interconnection flexibility for subsystem design and minimizes receiver complexity.

2) The interconnect scheme must accommodate transmission of data to all or most of the receiver terminals to allow broadcast transmission.

The report is organized as follows: it first reviews the state-of-the-art in interconnect technology, GaAlAs/GaAs lasers and transmitters, and GaAlAs/GaAs detectors and receivers. Analyses will then be provided of three different generic techniques for optically interconnecting optoelectronic circuits. Based on the requirements of high bandwidth and the known characteristics of GaAs detectors, optical interconnect schemes will be suggested. To interconnect IC's, this scheme will require the development of technology in several areas. Each of these areas will be treated separately, and the necessary development will be clearly identified. Finally, an assessment of technology for optically interconnected systems will be attempted, and a program plan to develop and implement optical interconnect will be presented.

2.0 ASSESSMENT OF CURRENT TECHNOLOGY

To put into perspective the prospects for optical interconnect technology, it is necessary to assess the state-of-the-art of existing interconnect technologies as well as of the individual components that will be used in an optical interconnect scheme. This analysis will provide the basis for subsequent evaluation of optical interconnect approaches and will identify the required technology development.

2.1 Interconnect Technology

At present, no developed interconnect technology exists that is suitable for interconnecting integrated circuits and systems which operate at frequencies in the range of two to five GHz. The majority of the available packaging/interconnect technologies are suitable only for low frequency multiple pin interconnects. Microwave packaging schemes are suitable only when a few ports or terminals are required. Examples of these two extremes are the packaging/interconnection schemes used for silicon VLSI circuits and the techniques used to interconnect GaAs transistors in very high frequency amplifiers. To achieve the interconnection of large densities of ports or terminals that operate at high frequencies will require innovative approaches in packaging and signal transmission. Many new approaches are being proposed to accomplish the interconnection of complex Si integrated circuits with support circuitry and other subsystems. Two examples of packaging approaches are shown in Figs. 1 and 2. While these packages accommodate the large number of terminals on the VLSI chip, they are designed to operate at frequencies no higher than 10 to 20 MHz. The extension to circuits operating at two to four GHz is not obvious. The spacing of the conductors will not support signal transmission at frequencies as high as one GHz.

Reduced coupling between parallel conductors can be accomplished if they are arranged in a strip line configuration with a common grounding plane. This approach has been utilized by Mayo Laboratories to successfully interconnect

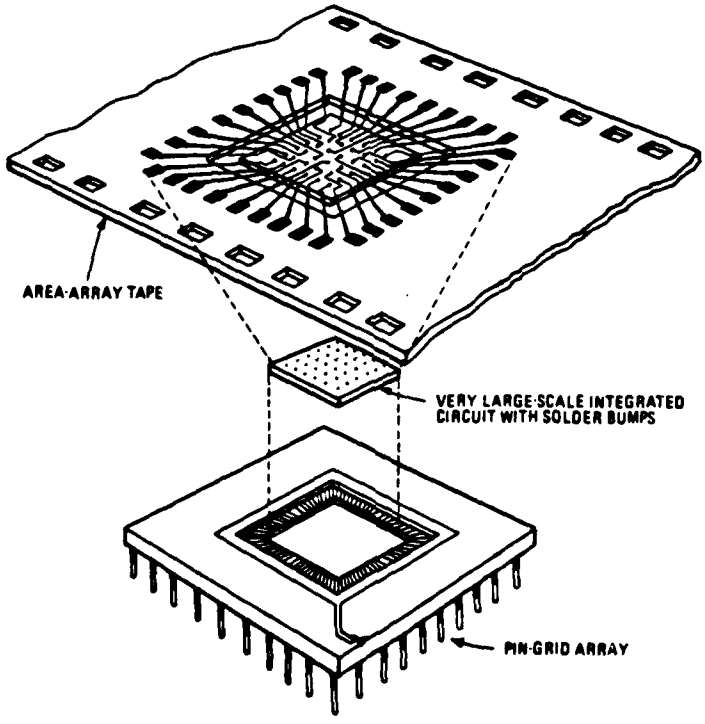
AREA-ARRAY TAPE
VERY LARGE-SCALE INTEGRATED CIRCUIT WITH SOLDER BUMPS
PIN-GRID ARRAY

Fig. 1

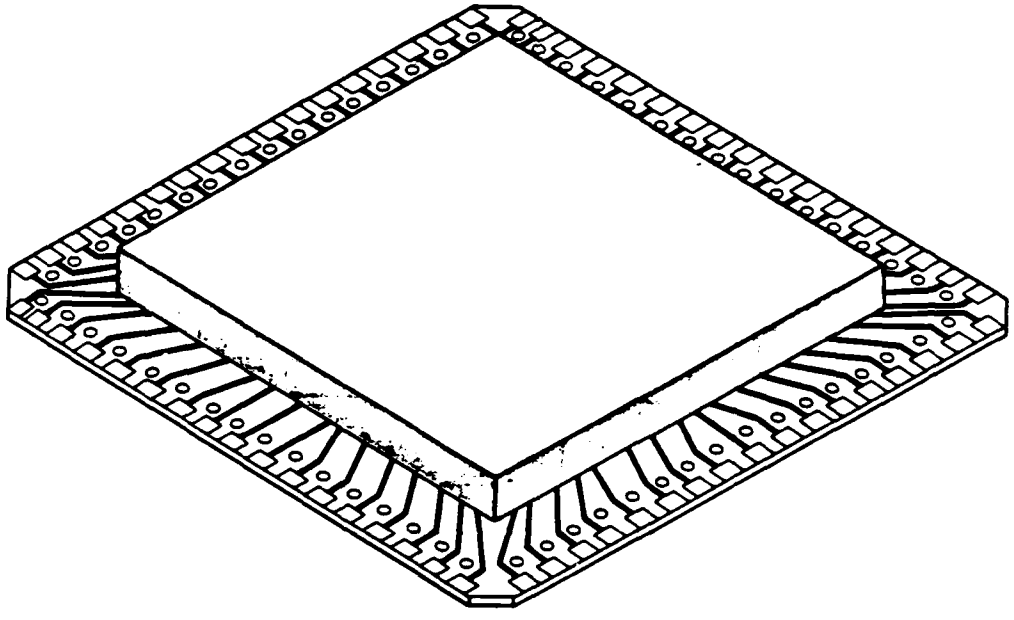

Fig. 2

ECL circuitry operating at frequencies as high as one GHz. Figure 3 shows a photograph of one such system. Strip line interconnect, however, requires careful termination of each line. The degree of fanout that would be necessary to accomplish broadcast interconnect of several ports is impractical. Furthermore, at frequencies as high as four GHz, significant coupling of signal between lines occurs for stripline separations as small as 100 μm. Unacceptable coupling occurs at these frequencies for separations in the range of usual GaAs pinout separations. Thus, the current interconnect technologies are unsuitable for the interconnection of GaAs integrated circuits. This is particularly true when one wishes to consider the broadcast interconnect of many circuits by the use of packet transmission concepts.

2.2 Laser Technology

The GaAlAs/GaAs double heterojunction injection laser will be the basis of the transmitter for any near-term high speed optical interconnect scheme. These lasers have demonstrated high performance, long life, and ready integration with a well developed integrated circuit technology based on GaAs. As a result, one can consider optical interconnect using laser transmitters at frequencies approaching four to five GHz. In this section, we will review the state-of-the-art of GaAlAs/GaAs lasers including threshold current, the dependence of threshold current on temperature, the high speed response, and the differential quantum efficiency of various laser designs.

One of the prime considerations in the use of GaAlAs/GaAs laser transmitter to interconnect integrated circuits will be power dissipation. The major controllable quantities in minimizing power dissipation are the threshold current of the laser and the differential quantum efficiency. These two quantities determine the quiescent operating point of the device as well as the operating current range for a particular system application. Thus, it is expected that minimization of the threshold current density and maximization of the differential quantum efficiency will be requirements of an optical interconnect scheme.

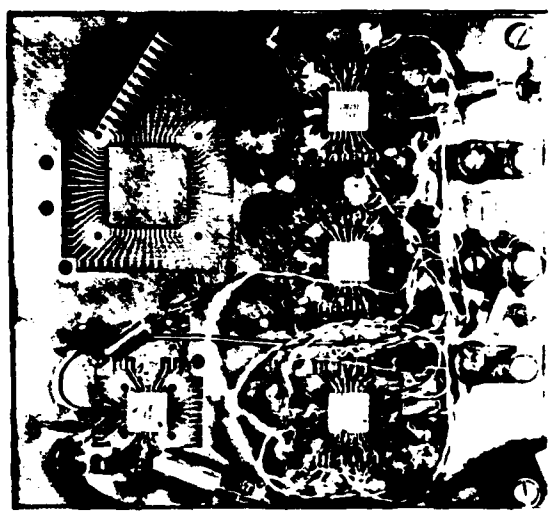

Fig. 3

A simple stripe geometry GaAlAs/GaAs laser in shown schematically in Fig. 4. The device consists of four layers grown on a GaAs substrate. The first three layers which alternate between GaAlAs and GaAs define an optical waveguide which confines the optical energy to the central GaAs region of the waveguide due to the lower index of refraction of the GaAlAs confining layers. The GaAlAs layers also serve another purpose. The n-type GaAlAs layer, because of its higher energy gap, serves as a carrier reflecting barrier that tends to confine carriers injected into the active region near the junction. Similarly, the p-type GaAlAs barrier layer serves as a wide bandgap emitter which suppresses electron injection back into the p-type GaAlAs. This has the effect of causing all current flow to be dominated by injection of holes into the n-type GaAs active region. The use of this structure has resulted in the extremely low threshold current densities of current GaAs lasers. Figure 5 shows the dependence of the threshold current density upon the active layer thickness, d.[1] Note that the threshold current density has a minimum value at an active layer thickness of approximately 700 to 800 Å. The data points shown on the figure represents the best values obtained by three different materials technologies for the various device parameters. There is generally good agreement between the experimental results and the theoretical calculations.

To achieve low threshold current devices, structures must be devised which maximize the confinement of the optical wave parallel to the junction and limit the total area of current flow. Several techniques to achieve this have been devised. Examples of them are shown schematically in Fig. 6. Structures in which the current is confined by an oxide or by proton bombardment typically result in confinement of the optical wave owing to a variation of gain across the active region-gain-guided lasers. By comparison, device structures which utilize active steps in the effective index of refraction across the active portion of the device are called index guided structures or mode controlled structures. A special case is the transverse junction stripe laser which relies on index guiding to confine the wave in the direction parallel to the junction but upon gain guiding to control the mode in the

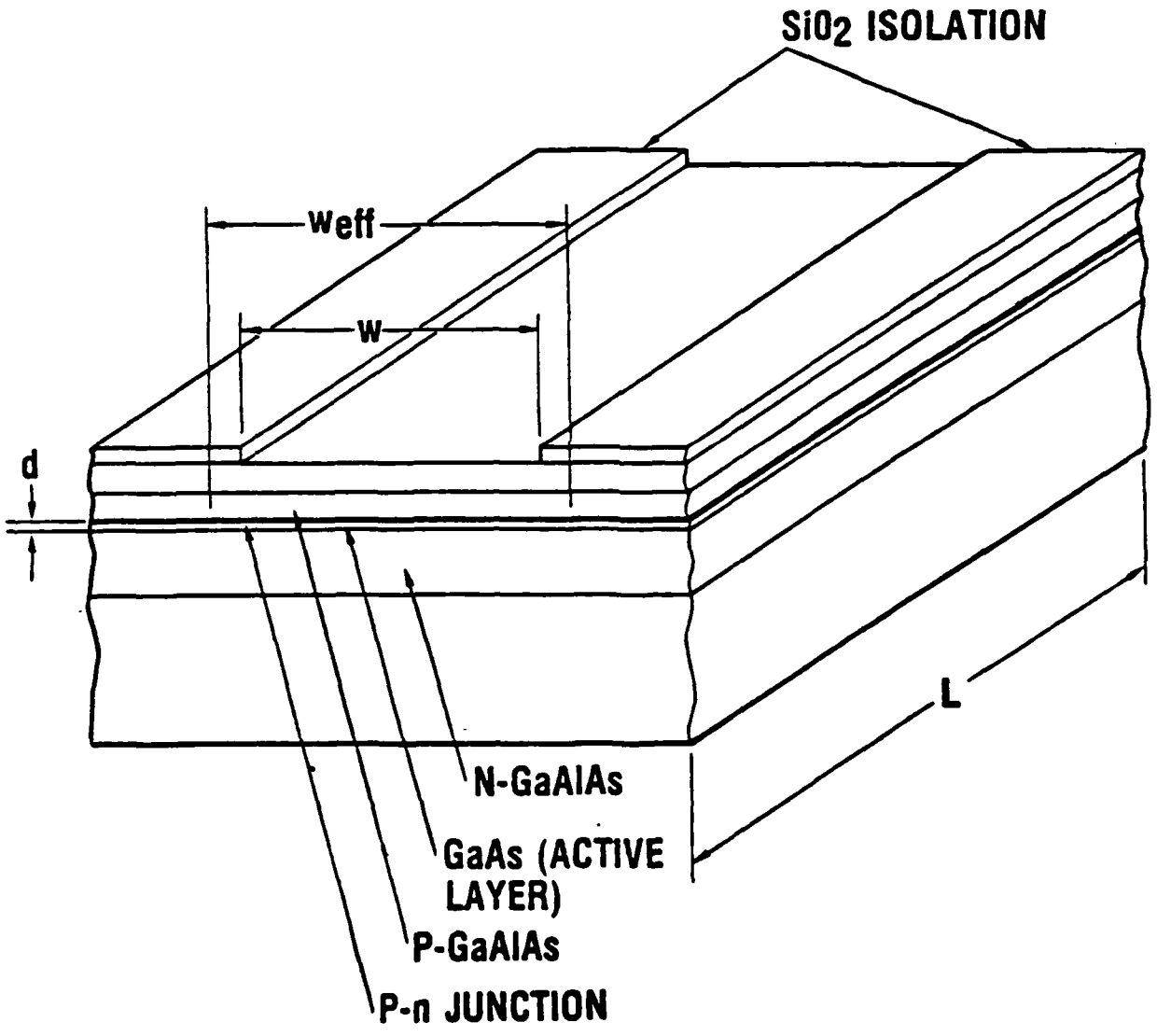
SiO2 ISOLATION
Weff
W
d
L
N-GaAlAs
GaAs (ACTIVE LAYER)
P-GaAlAs
P-n JUNCTION

Fig. 4

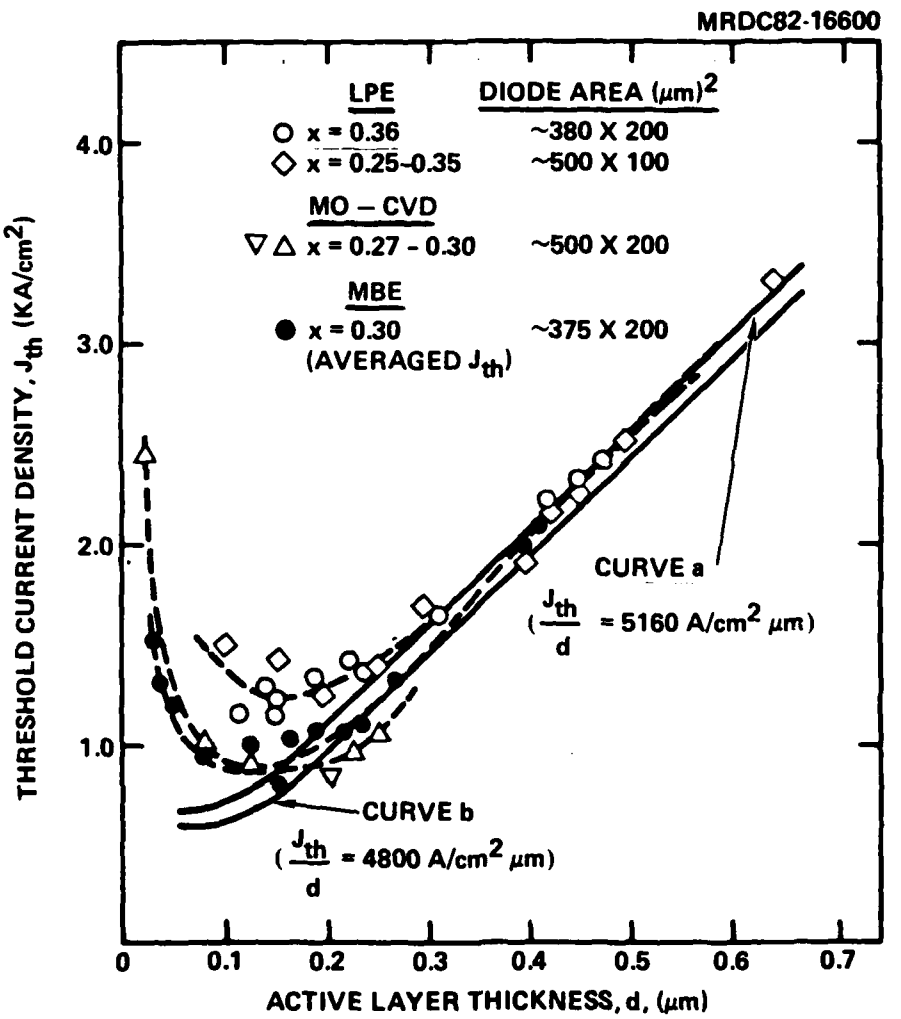
MRDC82-16600
LPE
DIODE AREA (μm)²
○ x = 0.36
~380 X 200
◇ x = 0.25-0.35
~500 X 100
MO – CVD
▽△ x = 0.27 - 0.30
~500 X 200
MBE
● x = 0.30
(AVERAGED Jth)
~375 X 200
CURVE a
(Jth/d = 5160 A/cm² μm)
CURVE b
(Jth/d = 4800 A/cm² μm)
THRESHOLD CURRENT DENSITY, Jth (KA/cm²)
4.0
3.0
2.0
1.0
0
0.1
0.2
0.3
0.4
0.5
0.6
0.7
ACTIVE LAYER THICKNESS, d, (μm)

Fig. 5

CROSS SECTION SCHEMATIC	STRUCTURE	I_{th} (mA)	T_o (K)	n_{ext}	f_{max} (GHz)	REF
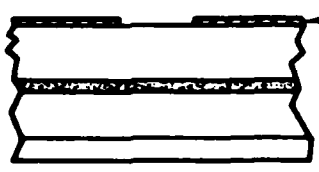	OXIDE STRIPE	70-100	140-170	40-50	1-2	2-3
	PROTON BOMBARDED STRIPE	30-100	140-170	40-70	1-2	4
	DEEP DIFFUSED STRIPE	70-100	120	40-80	5	5-6
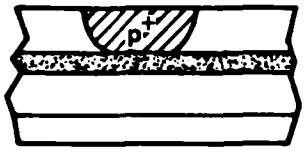	NARROW DIFFUSED BIPOLAR STRIPE	30-50	170	80-90	2-3	7
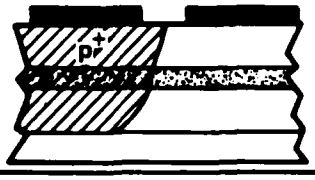	TRANSVERSE JUNCTION STRIPE	20-30	120	50	2-8	8-10
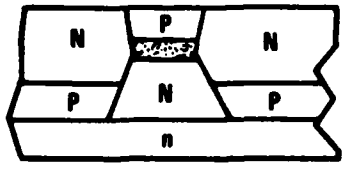	BURIED HETERO-STRUCTURE	10-30	120-170	80-90	1-3	11-17

P(N) – p(n) - TYPE GaAlAs
p(n) – p(n) - TYPE GaAs

ACTIVE REGION
DIFFUSED P^+ REGION

Fig. 6

direction perpendicular to the junction. Figure 6 also shows the lowest threshold current that has been obtained using each of the structures for nominal 200 to 300 μm long cavity.

Temperature Dependence of Threshold

Over the temperature range 0°C to 70°C, most double heterostructure lasers are dependent upon temperature as given in the following equation:

$$J_{th} = J_{th} \exp(T/T_0) \tag{1}$$

This empirically derived equation indicates that the threshold current can be a very strongly varying quantity with temperature depending upon the value of T_0. T_0 in turn depends upon a large number of device and technology parameters. However, the best and average values of T_0 for each of the device structures are listed in Fig. 7. In each case, the most common T_0 value for a double heterostructure laser independent of the lateral guiding mechanism is 150K to 180K. On the other hand, both the TJS device structure and the deep diffused device structure have T_0's in the range of 120K. This results from parallel current leakage in the GaAlAs regions of the diffused junction's structure. It appears to be fundamental to the device structures and is a distinct disadvantage of these two devices.

Frequency Dependence

Semiconductor laser operation involves a nonlinear interaction between the injected carrier density and the emitted photon population that strongly affects the frequency dependence of the device. Interaction between the photons in a laser mode and the active carrier density are governed by the following rate equations:[17-25]

$$\frac{dn}{dt} = \frac{J}{ed} - \frac{n}{\tau_{sp}} - g\, Sn^{\ell} \tag{2}$$

$$\frac{dS}{dt} = -\frac{S}{\tau_p} + \alpha V \frac{n}{\tau_{sp}} + Vg\, Sn^{\ell}$$

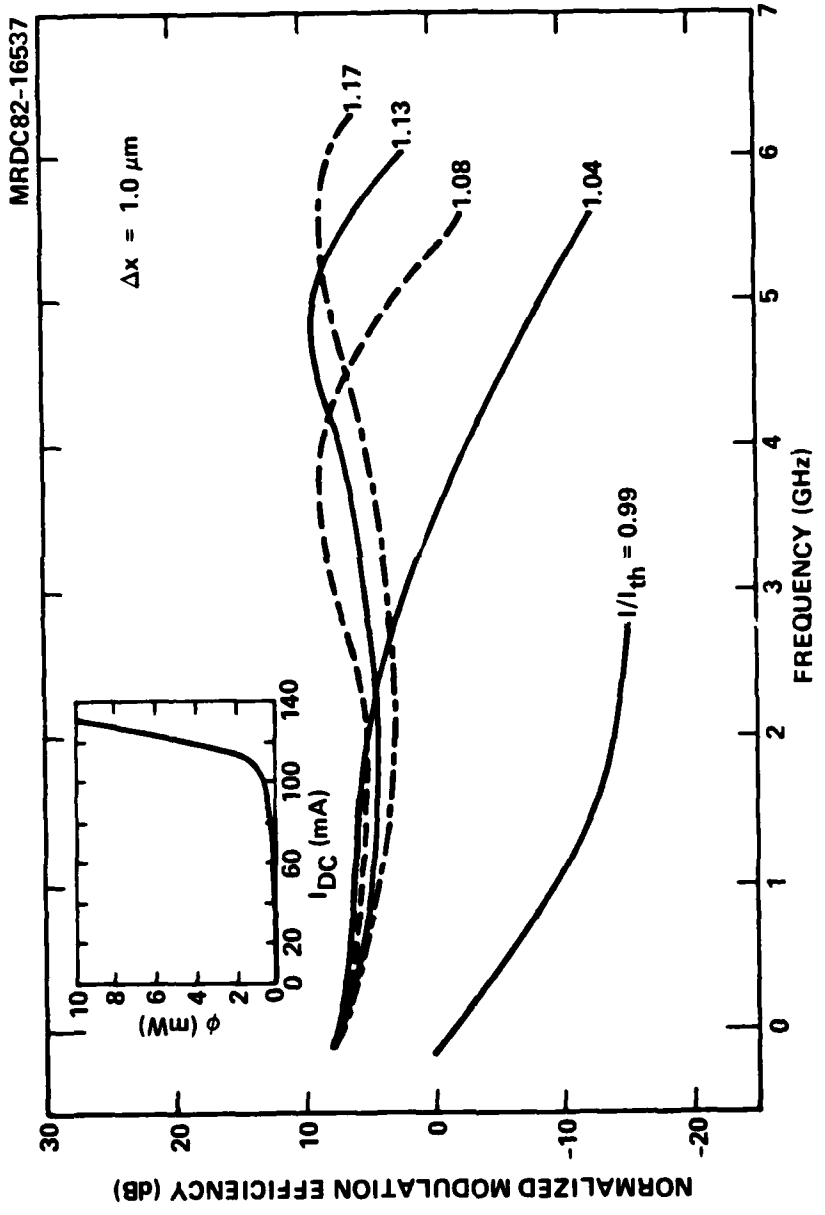
MRDC82-16537
Δx = 1.0 μm
1.17
1.13
1.08
1.04
I/I_th = 0.99
FREQUENCY (GHz)
NORMALIZED MODULATION EFFICIENCY (dB)
I_DC (mA)
φ (mW)

Fig. 7

where n(S) is the electron (photon) population; $\tau_{sp}(\tau_p)$ is the electron (photon) lifetime; g is the gain coefficient; V is the volume; and α is the fraction of spontaneous recombination emitted into the lasing mode.

These coupled nonlinear differential equations describe the simplest case of a uniform carrier and photon distribution in the semiconductor active region. Recent studies have shown that the effects of strong variations of either of these quantities within the active region can play a major role in modifying the frequency dependence of injection lasers. However, to describe the general characteristics of semiconductor lasers, we assume the uniform excitation case. To determine the frequency dependence of a semiconductor laser, we consider small signal modulation by a sinusoidally varying current.

Figure 7 shows the dependence of the modulation efficiency as a function of frequency for several different values of the DC current.[6] Several features are worthy of note. Below threshold, the frequency dependence shows a falloff above a critical frequency, $f_c[f_c = \frac{1}{2\pi}(\tau_{sp}\tau_p)^{-1/2}]$. Above threshold, there is a marked resonance in the modulation efficiency whose frequency increases with the drive current above threshold. The peak frequency of this resonance is given by the following equation:[20]

$$f_r = \frac{1}{2\pi}\left[\frac{1}{\tau_{sp}\tau_p}\left(\frac{J}{J_{th}} - 1\right)\right]^{1/2} = f_c\left(\frac{J}{J_{th}} - 1\right)^{1/2} \qquad (3)$$

Typical values for τ_{SP} and τ_p are 5 nsec and 2 psec respectively; this leads to a value for the characteristic frequency of $f_c \approx 1.5$ GHz. Thus, for operation at very high frequencies, biasing of the device well above threshold is required. On the other hand, higher frequency operation can also be achieved by reduction of the carrier lifetime or the photon lifetime. However, this usually results in an increase of the threshold current density. For example, a decrease by a factor of four in the photon lifetime or carrier lifetime results in a factor of two increase in f_c. On the other hand, these decreases will result in an increase of laser threshold and a decrease in differential quantum efficiency.

Several factors affect the height of the resonance including carrier diffusion,[19,25] nonuniform photon distribution,[19] and coupling between the carrier population and the spontaneously emitted photons in a particular mode.[20,26] However, for our purpose, it is important to note that the maximum frequency is determined to some extent by the drive conditions of the device and also by the device structure. Figure 6 also shows the best results obtained to date for the maximum frequency of operation, i.e., resonance frequency for each of the device structures.

The resonance peak exhibited in Fig. 7 also has a pronounced effect on the pulse response of these devices. The devices typically exhibit pronounced ringing at the onset and turnoff of pulsed operation due to this resonance phenomenon. The frequency of the ringing is equal to the resonance frequency. These relaxation oscillations can contribute a significant pattern effect when attempting to pulse code modulate laser devices at high frequencies. Several schemes have been devised to minimize such pattern effects. Adequate information is now available to reduce this to a manageable problem.

Differential Quantum Efficiency

The differential quantum efficiency of an injection laser is an important parameter for most applications. In the case of high speed pulse code modulation, the differential quantum efficiency and the bias dependence of the frequency response determines the average power required to achieve modulation at some given frequency. The laser will usually be biased near threshold to some quiescent operating point and then modulated with a current pulse above this operating point. The average current drive then is determined by these operating parameters and the system sensitivity. For most interconnect applications, the emitted power need not be more than 1 mW. However, it must be enough higher than the quiescent operating power to minimize the system sensitivity to noise. The differential quantum efficiency of various device structures is dependent upon the reflectivity of the laser mirrors and the internal losses of the device. The following equation gives

an expression for the external quantum efficiency in terms of the internal quantum efficiency:[27]

$$\eta_{ext} = \eta_{int}\left[\frac{\frac{1}{2L}\ln(\frac{1}{R})}{\frac{1}{2L}\ln(\frac{1}{R}) + \alpha}\right] \quad (4)$$

where L is the device length, R is the mirror reflectivity, α the loss coefficient and η_{int} the internal quantum efficiency. Device structures which minimize the coupling of the optical wave with the active region of the device typically have very high differential quantum efficiencies owing to reduced free carrier absorption losses. These structures can usually be obtained with very thin active regions and structures which are weakly confined in the lateral direction. However, the reduced coupling between the optical wave and the excited carrier density decreases the rate of stimulated emission and thus increases the threshold current. Figure 6 shows the highest differential quantum efficiency obtained with various device structures as well as the differential quantum efficiency observed at the lowest threshold current. In many cases, they are the same value. Clearly, differential quantum efficiency in the range from 40 to 90% can be obtained. The output power required for any particular application is usually determined more by the need to achieve low threshold or a certain speed of response.

Summary

A wide range of device structures exist which yield low laser thresholds, high speeds of response, and high differential quantum efficiencies. To permit laser operation at frequencies as high as four GHz or higher, it will be necessary to monolithically integrate the laser with the drive circuitry. This monolithic integration will probably be the guiding factor in determining which device structure is actually chosen.

2.3 Detector Technology

Monolithic integrated optoelectronics requires the use of GaAs detectors in the receiver portion of the interface. Although not as well

developed as Si detectors, GaAs detectors have shown performance characteristics which make them quite suitable for optical interconnect at very high data rates. In this section, we will describe the characteristics of GaAs photodetectors that have been reported.

Efficiency

GaAlAs/GaAs photodetectors have routinely been fabricated which achieve quantum efficiencies in excess of 80%.[28,29] This high quantum efficiency results from the use of a GaAlAs surface layer to minimize the loss due to the surface recombination of photo-generated carriers. GaAs has an absorption coefficient in excess of 10^4 cm^{-1} above its bandgap. As a result, for wavelengths of light which are efficiently detected (i.e., those above the bandgap of GaAs), the photo-generated carriers are generated within 1 to 2 μm of the surface. Thus, many of the photo-generated carriers can diffuse to the surface and recombine there if it is not properly passivated. This is accomplished by the use of the GaAlAs layer that serves to repel minority carriers from the surface and minimize surface recombination. Because of this barrier, most of the minority carriers generated in the material are available to diffuse to the junction and generate current within the external circuit. At Rockwell, we have been able to routinely fabricate GaAlAs/GaAs detectors with quantum efficiencies in the near infrared portion of the spectrum of 80% or greater. This should be more than adequate for the applications envisioned in this study.

Frequency Response

The frequency response of GaAs photodetectors is primarily limited by transit across the depletion width of the device. In a properly designed device, all of the absorption occurs within the depletion region, and the carriers are swept to the p-n junction by the built-in field of the junction. This is accomplished by designing the device with low enough doping on either side of the junction that the depletion width is greater than 2 μm in extent. As is shown later, when the device is operated near breakdown this corresponds to a doping level of ~10^{16} cm^{-3}. Law, et al,[29] have

demonstrated very high speed GaAs avalanche photodiodes with rise and fall times ~ 35 psec. The total pulse width for this device was ~150 ps FWTM. This device was constructed as a window photodiode with a very lightly doped p region that was biased to complete depletion or punch through. Under these conditions of operation, all of the photons are absorbed in the p-type GaAs portion of the device and are swept to the junction in the resulting built in field.

Gain and Leakage Currents

The leakage currents in GaAlAs/GaAs devices are typically dominated by surface currents. Thus, careful passivation of the surface is necessary to reduce the leakage levels to a minimum value. For devices with 100 μm diameter, the leakage currents can be made as low as one to two pA. This is more than adequate for high performance PIN and avalanche photodiodes. With leakage levels in this order, high gain avalanche photodiodes with high sensitivity have been fabricated at Rockwell. These devices exhibited gains of the order of 50 to 90 at operating voltages near 120 V. The system requirements based on an analysis of optical coupling characteristics will be described later. However, gains in the range from 10 to 100 appear to be adequate for most interconnect circumstances.

Capacitance

The capacitance of GaAs photodetectors is an important consideration in the design of high speed digital receivers. For example, in order to improve noise characteristics over a simple 50 Ω input impedance preamp, the transimpedance design may be used. However, with this design using a transimpedance of 1,000 Ω, the capacitance of the photodiode must be reduced to below 0.5 pf to achieve frequency response >1 GHz. Thus, the doping levels of the device and the area of the device must be designed to achieve these very low capacitance levels. Figure 8 shows the dependence of capacitance upon doping level for various levels of reverse bias. To achieve capacitances of ~0.5 pF or less in a 100 μm diameter device will require doping levels below 2×10^{16} cm^{-3} and reverse bias above 10 V and high reverse biases.

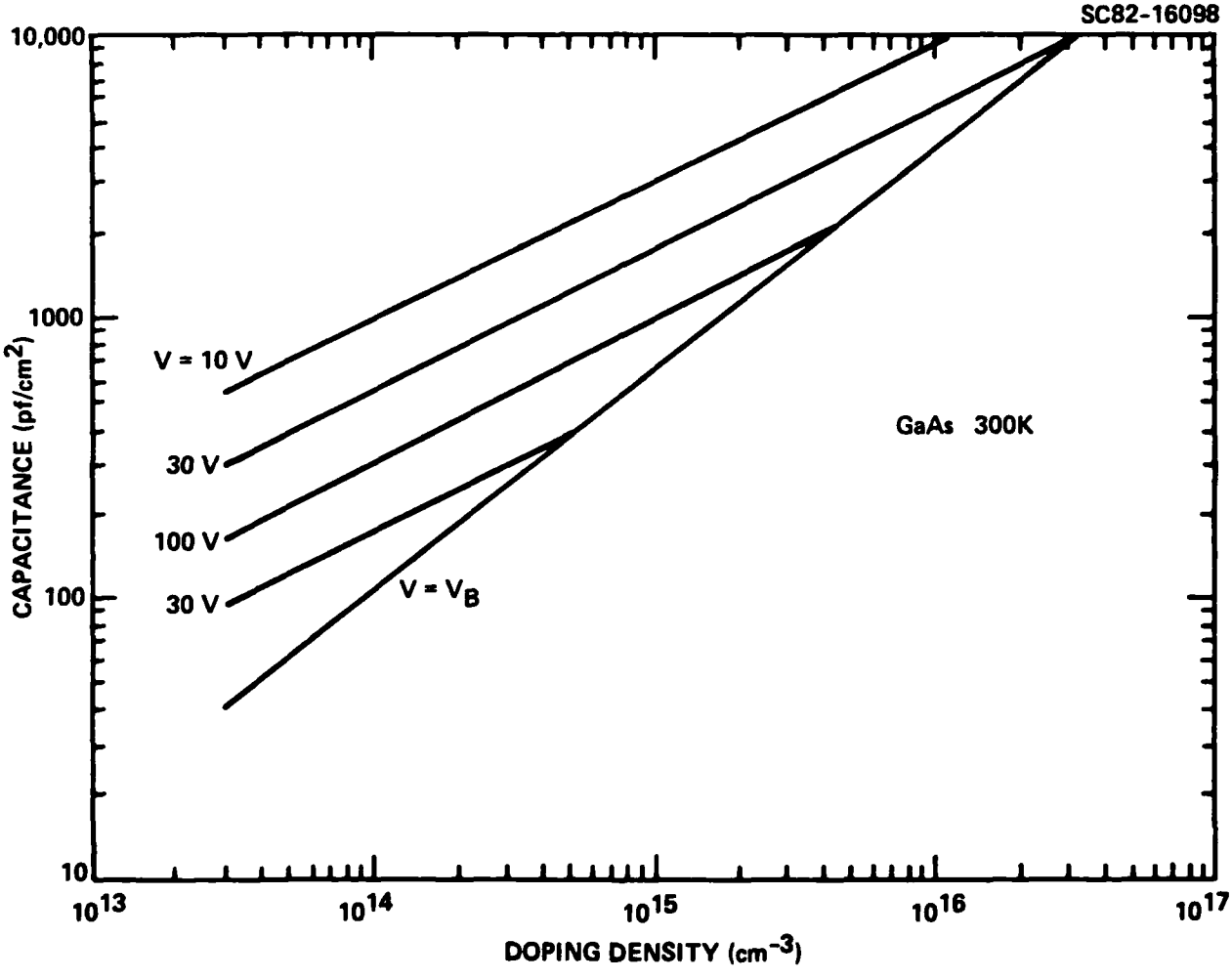
SC82-16098
10,000
1000
100
10
CAPACITANCE (pf/cm²)
V = 10 V
30 V
100 V
30 V
V = V_B
GaAs 300K
10^13
10^14
10^15
10^16
10^17
DOPING DENSITY (cm^-3)

Fig. 8

2.4 Integrated Optoelectronics

The integration of optoelectronic devices with electronic devices is at its very early stages of development. Early demonstrations[30-34] of integration have focused on feasibility rather than practicality, and performance required for interconnection of very high speed devices has not yet been demonstrated.

Monolithically integrated transmitters have been fabricated in a number of configurations. These transmitters typically consisted of a single drive transistor and a laser integrated on the same chip. Field effect transistors[30] (FET), bipolar heterojunction transistors,[31] and Gunn devices[32] have been integrated with GaAlAs/GaAs lasers. However, the configurations of all of these demonstrations have been such that high speed performance or even high efficiency performance have not been attempted. The major drawbacks to these designs have been that the lasers and the drive transistors have been fabricated with too coarse a geometry to allow high speed modulation. The highest modulation speed was obtained with a transmitter in which a laser and FET were vertically integrated.[33] However, this transmitter design is not practical for application to interconnect and has been abandoned in favor of the planar approach chosen by Rockwell and presently being developed under a separate DARPA contract. The Rockwell approach (see Fig. 9) utilizes the well-developed GaAs integrated circuit technology along with advanced materials technology to create a planar integrated optoelectronic technology that will be capable of very high speed operation. Operation at frequencies as high as four GHz will require the use of FET drivers with 1 μm or less gate lengths that can only be defined on surfaces that are smooth and planar. The mesa approach characteristic of early integration attempts is not suitable. Rockwell's approach is to grow the epitaxial layers for the double heterostructure laser in a groove on the surface of the semi-insulating substrate. This results in a planar substrate surface for subsequent ion implantation and fine line lithographic definition. To date, Rockwell has demonstrated the operation of lasers on semi-insulating substrates as well as the operation of high speed FET's and transferred electron devices on substrates on which lasers have been grown. Efforts to achieve laser operation with on-chip drivers are now in progress.

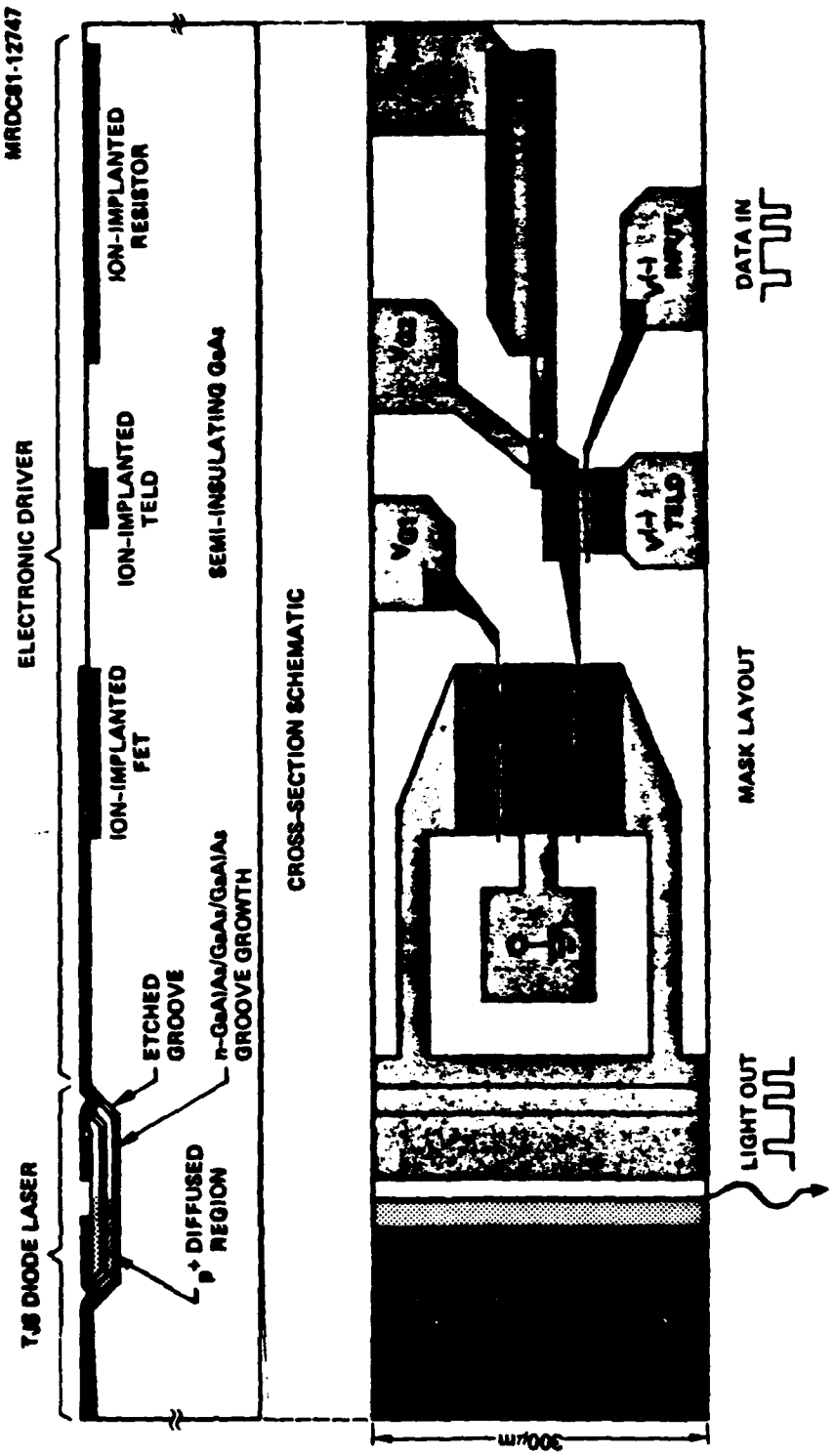
MRDC81-12747
ELECTRONIC DRIVER
ION-IMPLANTED RESISTOR
ION-IMPLANTED TELD
SEMI-INSULATING GaAs
ION-IMPLANTED FET
n-GaAlAs/GaAs/GaAlAs GROOVE GROWTH
ETCHED GROOVE
DIFFUSED REGION
T-J DIODE LASER
CROSS-SECTION SCHEMATIC
DATA IN
LIGHT OUT
MASK LAYOUT
300μm

Fig. 9

Integrated receivers for the most part have taken the form of photodiodes monolithically integrated with a low noise FET. These useful demonstrations of integration, however, were not aimed at high speed performance, and thus the fine line geometry and the low capacitance were not demonstrated. On the other hand, Yariv and coworkers[34] have demonstrated a monolithically transceiver consisting of an FET detector, an FET driver, and a laser on the same chip. No high speed performance was attempted.

These early attempts at integration represent the beginning of what must become a concerted development program to integrate the epitaxial technology for optical devices with the ion implantation technology for electronic devices. At present, the lasers transmitters, for example, all are fabricated using cleaved mirror lasers. This choice of laser cavity automatically limits the dimensions of the transmitter. In order to build field effect transistors with the required drive power to operate lasers, one must establish a rectangular geometry for the transmitter chip. This is dictated by the need to place the FET and the transferred electron logic device (TELD) in close proximity to the laser without making the cleaved laser too long to be practically driven by an FET. In turn, this requires that the laser be > 300 μm long. Longer lasers will have too high a threshold, and shorter lasers will make it impossible to fabricate the necessary electronic drive devices close enough to the laser. Tradeoffs such as these are only now being addressed. These and similar questions must be answered before a monolithic integrated optoelectronic technology is ready for application to IC interconnect.

3.0 ASSESSMENT OF OPTICAL INTERCONNECT

Interconnection of high speed digital integrated circuits utilizing optical means requires that a passive optical distribution network must be utilized to transmit the optical information from one point to another. To permit the general interconnection of one transmission point with other reception points in the system, we assume that the data are transmitted in a data packet from the various transmitters. As a result, the information is contained in a burst of bits, some of which indicate the destination, others the sender, and others the data to be transmitted. The transmission can be point to point or broadcast interconnect in which a given transmitter sends to all other receivers. As a result, it is required that the optical interconnect medium permit the efficient distribution of the optical energy to all of the required ports, with minimal loss due to coupling and insertion of the optical signal. Furthermore, the size of this optical medium and any network that may be involved must be compatible with the sizes of typical GaAs integrated circuits (1 cm) and projected systems utilizing such circuits (10 cm x 10 cm). The medium must be capable of transmitting signal over the required distances (10 cm) with sufficiently low dispersion to allow for four GHz data transmission.

In this section, we investigate three generic techniques for optically interconnecting integrated circuits - guided wave interconnect, broadcast interconnect, and high Q cavity interconnect. We will investigate the fanout and insertion losses of each of these generic techniques and consider specific examples of the ways in which these types of interconnect could be implemented. We will further investigate the possiblility of any dispersive effects that will limit the data handling capability of the media.

3.1 Guided Wave Interconnect

Guided wave interconnect refers to the transmission and distribution of optical data via a medium that localizes the optical energy and distributes

it to the required destination points. The two most obvious examples of guided wave interconnect would be optical fibers and planar wave guides. The interconnection of integrated circuits using optical fibers requires the hybrid coupling of the fibers to the transmitters and the receivers. An example of an optical interconnect approach that could be applied to the interconnection of integrated circuits is shown in Fig. 10. Here we show a biconical fused taper coupler[35-37] in which a large number, N, of optical fibers is fused at a point such that the injection of an optical signal in one of the fibers results in the distribution of the light energy to all of the output fibers in the bundle. A feasible implementation of a biconical fiber coupler is shown in Fig. 11. Here the fiber network is coupled to both the lasers and the detectors from the top surface of the device. Alignment between individual lasers and detectors is achieved by imbedding the fiber network in a precisely machined block that holds the fibers over the transmitters and receivers. We will investigate the properties of this coupler as a generic example of guided wave interconnect.

The properties of biconical fused taper couplers[35,36] have been investigated in some detail. To achieve high efficiency coupling from the input port to all of the output ports, it is necessary to arrange the fibers in a close packed configuration during the fusion process, so that maximum surface contact between the various fibers is achieved. In this manner, workers have fabricated couplers with 1, 7, and 19 fibers.[35,36] The operation of these couplers results from the radiation of the power in the input fiber into the cladding layers of the fiber bundle, owing to the taper in the core of the input fiber and the subsequent capture and transmission of this radiation in the output fiber cores. A relatively simple expression for the coupling between an input fiber and an output fiber has been developed.

$$C_{ij} = \frac{K_r K_t}{N} \tag{5}$$

where C_{ij} is the coupling between the i^{th} input fiber and the j^{th} output fiber, K_r is the fraction of the incident power radiated into the cladding, K_t

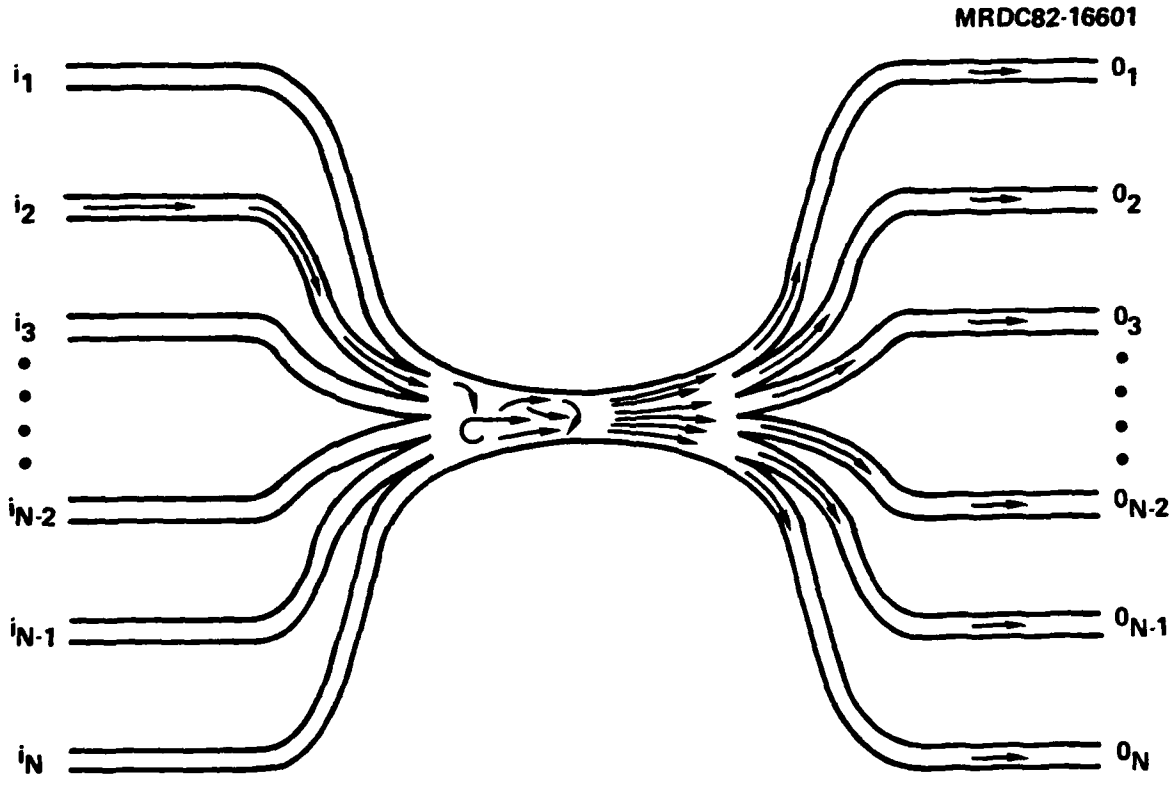

Fig. 10

MRDC82-16602

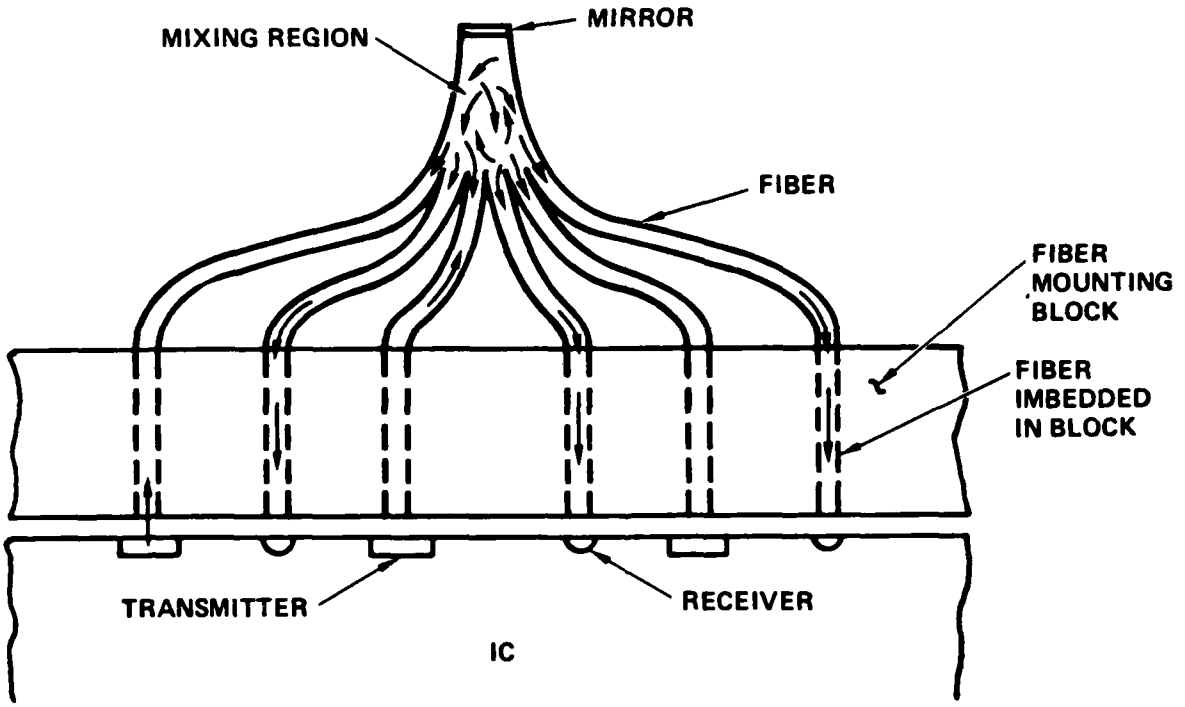

Fig. 11

is fraction of the radiated power reabsorbed into the output fiber, and N is the number of fibers in the taper coupler. Similarly, the coupling coefficient for the i^{th} input fiber and i^{th} output fiber can be expressed as

$$C_{ii} = (1 - K_r) + \frac{K_r K_t}{N} \tag{6}$$

The total efficiency of the coupler, K_e, is

$$K_e = C_{ii} + (N - 1)\, C_{ij} \tag{7}$$

$$K_e = C_{ii} + \sum_{j \neq i} C_{ij} \tag{8}$$

In Fig. 12, we show the coupling coefficient C_{ij} vs the number of fibers in the fiber coupler on a log-log plot. Notice that the experimental data agree well with the expression given in Eq. (5) if the empirical values of 0.6 for K_t and 0.85 for K_r are used. The insertion loss of the coupler is given by the product $K_r K_t$. This is equal to 50% or 3 dB. The important result to be derived from this figure, however, is that the use of an optical fiber distribution network will result in the splitting of the optical energy into N approximately equal parts and the subsequent distribution of these parts to N ports.

The coupling of light between points via guided waves can also be accomplished by the use of planar waveguides in an optically transparent medium. Several technologies have emerged which will allow the low loss coupling of energy from one point to another via optical waveguides. Two of the most promising technologies involve the use of diffused waveguides in lithium niobate and laser annealed waveguides[38,39] in deposited glass waveguides on silicon substrates. In the latter case, waveguide losses as low as 0.60 dB/cm have been achieved.[39] While significantly higher than for glass fibers, this loss still represents a major achievement in the technology of

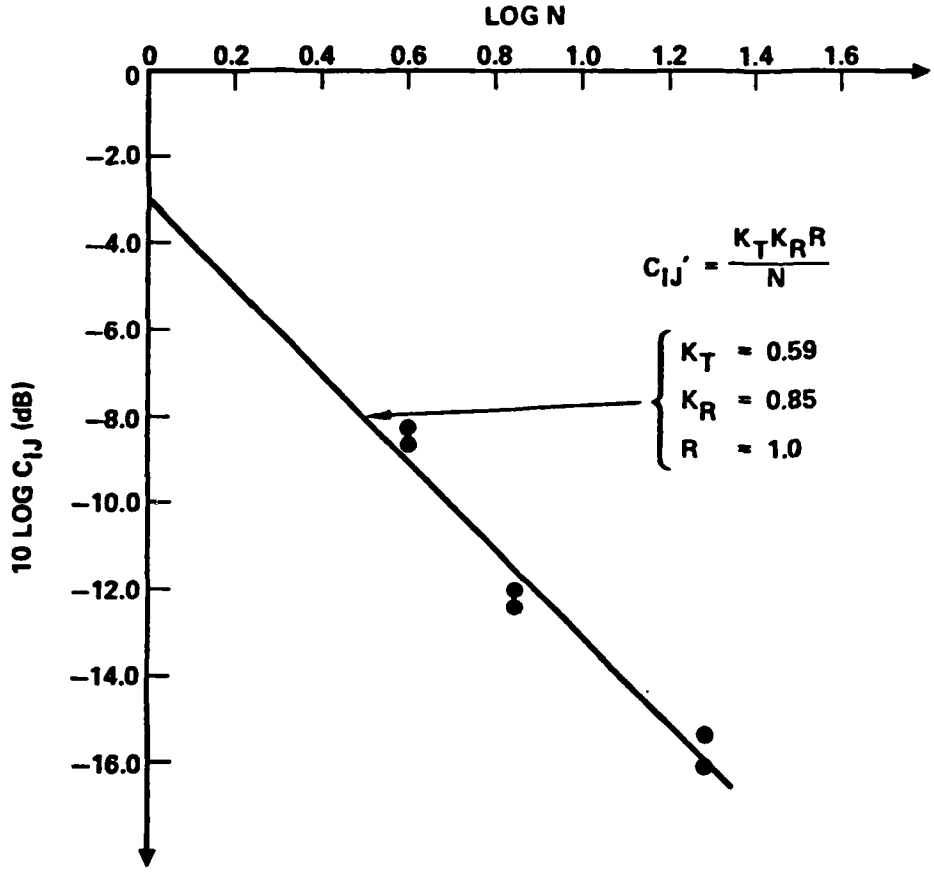
LOG N
0
0.2
0.4
0.6
0.8
1.0
1.2
1.4
1.6
0
-2.0
-4.0
-6.0
-8.0
-10.0
-12.0
-14.0
-16.0
10 LOG C_{IJ} (dB)
$C_{IJ}' = \frac{K_T K_R R}{N}$
K_T = 0.59
K_R = 0.85
R = 1.0

Fig. 12

optical waveguides. By contrast, the usual losses in lithium niobate type waveguides is of the order of one to two dB/cm. As a result, transmission over 10 cm will result in a signal decrease by an order of magnitude or more. This could reduce the system sensitivity in a large area system. However, the losses in glass waveguides have reached the point where planar waveguides appear to be reasonable interconnect technology for high speed integrated circuit. One difficulty of using planar waveguides is the need to accommodate the necessary bends in the waveguide in a small area to allow the distribution of the light to the various ports. Typical bend radii for planar waveguides are of the order of two cm. This is a relatively large geometry compared to a 10 cm board and may render planar waveguide interconnect useless for some circuit interconnects. The distribution of optical energy in a planar waveguide will result in a 1/N distribution. However, the insertion losses will be considerably reduced, since the coupling between adjacent waveguides results in little or no loss of radiation.

To summarize and assess guided wave interconnect, we must consider all of the losses that will occur in transmission of a signal from one laser to one detector on a large area circuit board. These losses include the wave guide insertion losses (that is, the efficiency of coupling light from the laser into the guide), coupler insertion losses, the splitting losses that result from splitting the energy into N roughly equal parts, and finally any absorption or scattering losses that might occur in the waveguide during the transmission of the energy. It is expected that the latter losses will be minimal or zero in commercial optical fibers but may become substantial in planar waveguides where corner turning can result in substantial radiation losses.

3.2 Broadcast Interconnect

The second technique for interconnecting various ports of a high speed integrated circuit system involves the broadcast transmission of the optical energy in free space. Since we envision the circuits all packaged on

a planar substrate, broadcast interconnect must be accomplished via the spatial dispersion of the optical signal from an overhead source, such as shown in Fig. 13. Here the optical radiation is aimed at a highly diffusing but highly reflecting surface. This surface results in the reflection of the optical signal in a Lambertian distribution. This form of interconnect has the advantage that there are virtually no insertion losses, and the major loss results from the fractional area subtended by the detector compared to the illuminated area. This can be quantified by considering the geometry considered in Fig. 13. Here we consider a transmitter radiating light in a very narrow beam onto a perfectly rough and perfectly reflecting surface. As a result, the light is dispersed in a Lambertian distribution and is broadcast over a large area. If the detector sits at a distance, R_j, from the transmitter, the intensity of light received by the detector can be estimated from classical physical concepts. If the area of the receiver is A_r and it is situated at a distance, X, from a transmitter in the cavity as shown in Fig. 13 with a height, H, the intensity of light received by that receiver can be expressed by the following equation:

$$I = \frac{I_o}{4\pi} \frac{A_r}{(x^2 + H^2)} \cos^2 \phi = \frac{I_o}{4\pi} A_r \frac{H_2}{(H^2 + X^2)^2} \tag{9}$$

Since the $\cos^2\phi = H^2/(X^2 + H^2)$, the fraction of the intensity received at a point R from a transmitter can be expressed as shown in the second equality. If we normalize those quantities by the maximum distance over which the light would have to travel from one corner of a circuit board to another, X_{max},

$$I = \frac{I_o}{4\pi} \beta \frac{h^2}{(x^2 + h^2)^2} \quad . \tag{10}$$

where

$$\beta = \left(\frac{A_R}{X^2_{max}}\right), \; h = H/X_{max} \text{ and } x = \frac{X}{X_{max}}$$

MRDC82-16603

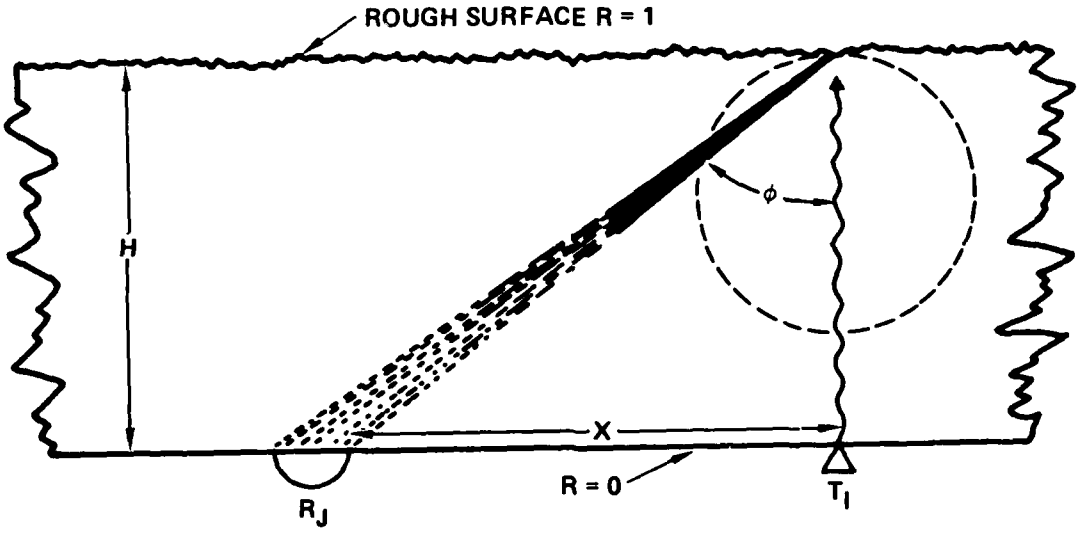

Fig. 13

From this expression, it can be seen that the coupling efficiency, I/I_0, varies as the ratio of the detector area to the area being illuminated. This ratio, β, is the determining factor in deciding the area coverage possible with broadcast interconnect. The other terms which represent the geometric fraction of the Lambertian source subtended by the detector can be made a slowly varying function of position on the board. This is shown in Fig. 14 where we plot the relative intensity normalized to β as a function of position for various ratios of the height of the coupling container to the total dimension to be illuminated. Clearly, for values of the height equal to or greater than the dimension to be illuminated, the dependence of this geometrical factor is small. This puts a constraint on the dimensional size of the package to be utilized for radiation coupling. Thus, to interconnect circuits on a 10 cm x 10 cm circuit board, an enclosure whose height is 10 cm will be required. On the other hand, if the chips can be arranged on the circuit board such that communication is only necessary between one chip and its nearest neighbors, it may well be possible to use much smaller package heights. From Section 2.3, we know that large materials penalties will be paid to achieve very high data rates if the detector area is greater than 10^{-4} cm^2. Thus, to illuminate a 10 cm board with any chip on the board will require a minimum signal loss of 60 dB. This loss varies reciprocally with the square of the dimension of the board. If the area of the detector can be made larger, of course, this loss scales linearly with the area.

3.3 High Q Cavity Coupled Interconnect

As seen in the previous section, broadcast interconnect results in large losses owing to the small area subtended by a detector compared to the area being illuminated. Guided wave interconnect requires careful coupling of the radiation into the waveguide and has inherent coupling losses and increased fabrication difficulties. As a result, we have investigated a third type of interconnect scheme which we call high Q cavity coupling. In this scheme, all transmitters emit their radiation into a cavity with an extremely high Q; that is, there is minimal absorption loss on the walls of the cavity,

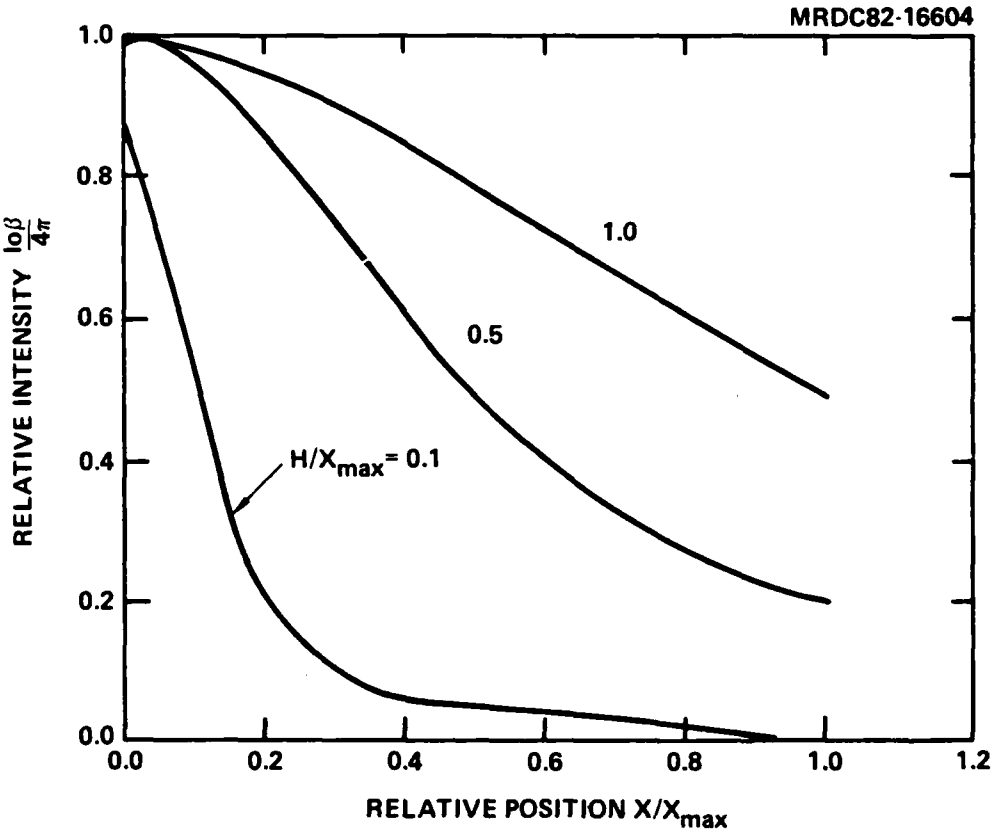
MRDC82-16604
1.0
0.8
0.6
0.4
0.2
0.0
RELATIVE INTENSITY $\frac{I_0\beta}{4\pi}$
1.0
0.5
H/X_{max}= 0.1
0.0
0.2
0.4
0.6
0.8
1.0
1.2
RELATIVE POSITION X/X_{max}

Fig. 14

and the major source of loss in the cavity is absorption by the receivers themselves. Ideally, under these circumstances, one can achieve the 1/N splitting of the radiation to the various receivers while at the same time minimizing the difficulties of signal insertion coupler fabrication. The model that we used to analyze this type of interconnect is shown in Fig. 15. To achieve good coupling or radiation from one transmitter to all possible receivers, the following conditions must be met by the high Q cavity. First, the reflectivity of the cavity must be extremely high, approaching one. There must be a region of the surface which randomizes the direction of the photons, or else the photons will merely establish a regular bounce pattern within the cavity. Thirdly, the mean free path of photons within this cavity, $\langle \ell \rangle$, must be

$$\langle \ell \rangle \gg V^{1/3}$$

where V is the volume of the cavity. This is to ensure that photons have a high probability of encountering at least one of the receivers.

To analyze this cavity coupling scheme, we employ the random photon gas model of Joyce.[40] This model was originally developed to account for radiation distribution in optical cavities with varying degrees of loss on the surface. Examples of this are light emitting diodes, integrating spheres, and various types of illumination systems. If the only two sources of loss in a high Q cavity are losses due to the absorption of photons at the receivers, each of which has an area A, and loss by absorption on the walls of the cavity due to the imperfect reflectivity of the cavity walls. If our cavity has a volume, V, and a surface area, S, the probability of loss can be expressed by the following equation:

$$P_t = \frac{nA}{S} + \left(1 - \frac{nA}{S}\right)(1 - \eta_R) \qquad (12)$$

The mean free path of a photon in the cavity is defined as:

HIGH Q CAVITY COUPLING

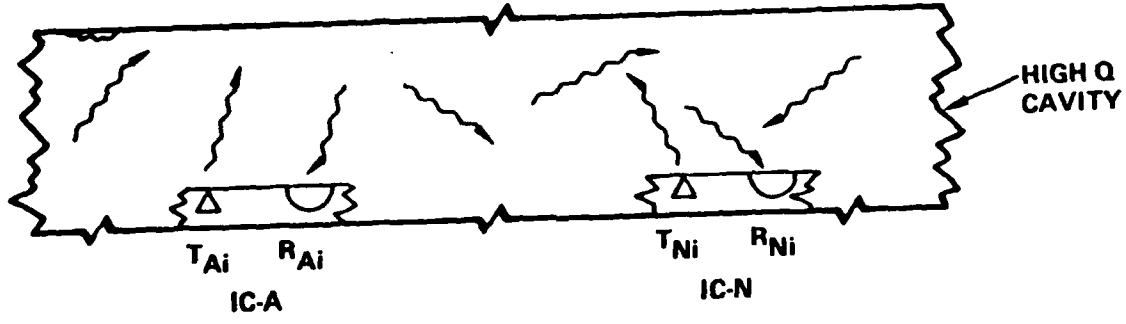

- HIGH Q CAVITY REQUIRED ⟹ MEAN FREE PATH >> $(V)^{1/3}$
- RANDOMIZING SURFACE REQUIRED ⟹ EFFICIENT COUPLING

Fig. 15

$$\langle \ell \rangle = \frac{4V}{S} . \tag{13}$$

This is the mean distance that a photon will travel before encountering a surface and being reflected or absorbed. Most photons will encounter many surfaces and be reflected many times before finally being absorbed or lost to the photon population within the cavity. The mean distance to loss, ℓ^*, is given by the following expression:

$$\ell^* = \frac{\langle \ell \rangle}{P_t} \tag{14}$$

This quantity describes the mean distance that a photon will travel before it is absorbed by either the cavity walls or a receiver. $(\ell^*)^2$ then represents the area coverage provided by the cavity coupling from a randomly located transmitter. One can represent the distribution of intensity of light from a transmitter by the following equation:

$$I \approx I_{oe}^{-x/\ell^*} \tag{15}$$

Using the above definitions, we can now define the mean photon lifetime or the mean time that a photon spends in bouncing around in the cavity before being absorbed. Thus, if a photon travels a mean distance, ℓ^*, before loss and travels at the speed of light, c, its time of existence is given by τ^*.

$$\tau^* = \frac{\langle \ell \rangle}{P_t c} \tag{16}$$

If a transmitter emits a burst of light at some time t = 0, there will be a significant fraction of this radiation still traversing the interior of the cavity and striking detectors, until most of the photons have been absorbed. To ensure minimal interference from the previous pulse, pulses must then be

separated by at least the time equal to the mean photon lifetime, τ^*. Thus, the frequency response of the cavity, f_τ, is given by the following equation:

$$f_\tau = 1/(2\pi\ \tau^*) \tag{17}$$

This gives the maximum frequency or bit rate which can be transmitted in such a cavity. Clearly, within the constraints of this frequency response or reverberation time, a high Q cavity will split the radiation from any transmitter equally between the various receivers. If the reflection of the cavity walls are the major source of loss, the insertion loss in this situation is given by the ratio of the number of photons that are absorbed by detectors to the number of photons that are absorbed on the cavity walls. This is given by the quantity R_C.

$$R_C = \frac{A}{S - NA(1 - \eta_R)} \tag{18}$$

This insertion loss is a very large number unless the cavity reflectivity is very high. Figure 16 shows the maximum frequency response of a high Q cavity as a function of geometrical factors within the cavity, calculated for a 10 cm cavity. Also plotted is the mean distance before loss within such a cavity. The maximum of frequency is denoted by the solid lines, and the mean distance before loss is denoted by the dashed lines. It is clear from the solid lines that in order to achieve frequencies in excess of 3 GHz, it will be necessary to have substantial losses in the walls of the cavity. That is to say the reflectivity must be less than 95%. Furthermore, the cavity must have a height to width ratio of greater than 1:10. Thus, in order to achieve a high data rate within the cavity, it will be necessary to minimize the distance that the photon travels and the time that the photon is alive within a cavity. This is accomplished by reducing the reflectivity of the wall and by increasing the number of encounters of the photon with the walls. However, under the same regime, the mean distance before loss in such a cavity is found

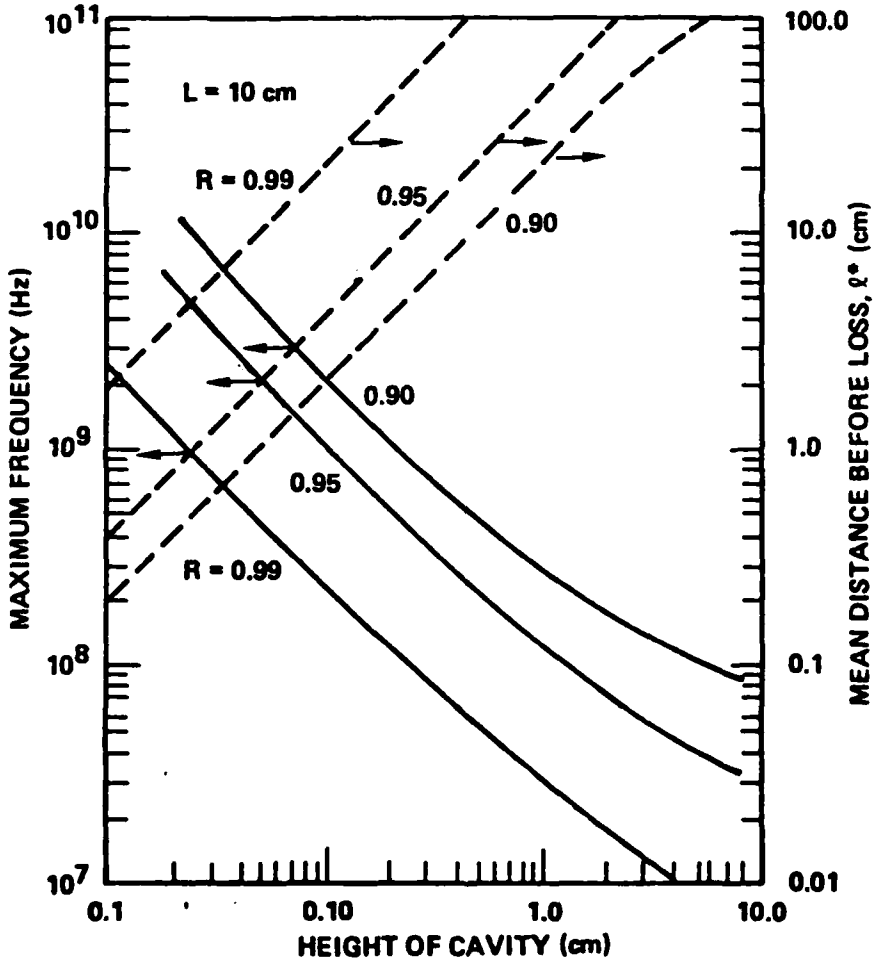
L = 10 cm
R = 0.99
0.95
0.90
0.90
0.95
R = 0.99
MAXIMUM FREQUENCY (Hz)
MEAN DISTANCE BEFORE LOSS, ℓ* (cm)
HEIGHT OF CAVITY (cm)
10^11
10^10
10^9
10^8
10^7
100.0
10.0
1.0
0.1
0.01
0.1
0.10
1.0
10.0

Fig. 16

to be much less than the area dimension of the cavity. For example, for a cavity height of 0.1 cm and reflectivity of 90%, one would expect a frequency response of the order of three GHz. By the same token, the mean distance before loss in such a cavity would be approximately 1 cm. Clearly, it would not be possible to interconnect a chip on one side of a board with a chip on the other side of the board using such a scheme. Thus, high Q cavity coupling is capable of providing a relatively high coupling efficiency, provided that the frequency or the data rate desired is below one GHz. However, for the general problem of interconnecting GaAs integrated circuits, it appears that high Q cavity interconnect is not suitable.

3.4 Receiver Considerations

We have examined in the previous sections three generic optical coupling approaches for the interconnection of integrated circuits. Of the three, only one high Q cavity coupling appears not to be a reasonable interconnect scheme for GaAs integrated circuits due to the limited frequency response inherent with that coupling scheme. In order to evaluate the suitability of broadcast and guided wave interconnect for the majority of the applications, we will now analyze the performance of state-of-the-art GaAs based optical receivers. The most important parameter to determine the suitability of any portion of an optically interconnected system, it is the signal-to-noise ratio of the receiver. For detector with quantum efficiency, n, operating at a gain, M, the optical signal current is given by[41]

$$I_p = \frac{qnPM}{h\nu} \tag{19}$$

For PIN detector, M = 1, and for an avalanche photodiode M can range from anywhere from 1 to 90 in the GaAs technology. A typical value for the quantum efficiency is 90%.

The avalanche multiplication process that multiplies the generated signal current also affects the noise generated in the photodiode. In addition to multiplying the noise currents by M, most avalanche photodiodes are found to generate an excess noise which is generally characterized by an excess noise ratio, F_p. For GaAs photodiodes, F_p is equal to $M^{0.7}$. The well known expression for the square of the noise currents is given by the following equation:(41)

$$I_n^2 = B\ (I_p + I_d)\ M^{2+xn} + 4\ KT/R \tag{20}$$

Thus we can define the signal-to-noise ratio as I_p^2/I_n^2, and this is given by the following equation:(41)

$$\frac{S}{N} = \frac{(\frac{q\ \eta PM}{h\nu})^2}{B(I_p + I_d)\ M^{2+xn} + \frac{4kT}{qR}} \tag{21}$$

For a typical APD receiver, the bandwidth, B, is determined by $(1/2\pi)\ (R\ C)^{-1}$ where R is the input resistance of the amplifier and C_n is the total input capacitance of the receiver. The effective noise current of the receiver is predicted to vary as $\alpha = (1 + 8 \times 10^{-12})\ B$. Typical input capacitance of a GaAs monolithic receiver is expected to be on the order of 0.5 pF. In the calculations that follow, R is varied to result in the required bandwidth. Typical leakage currents, I_d, for GaAs detectors vary in the range from 10^{-9} A to 10^{-12} A.

The minimum exceptable signal-to-noise ratio for most applications is a signal-to-noise ratio of one. For most practical systems applications, a signal-to-noise ratio of 10 or 100 is more likely required. We calculate the minimum power required as a function of the bandwidth to achieve a signal-to-noise ratio of 1 and 100. These are shown in the next two figures for a variety of values of the gain, M. Note that for a signal-to-noise ratio of one, the minimum average optical power necessary to achieve a signal-to-noise ratio of one occurs at a gain of approximately forty. Furthermore, it is

observed that the minimum optical power increases as the square of the bandwidth for all values of gain. At frequencies above three GHz, a minimum optical receiver power of ~45 dBm is required. For a signal-to-noise ratio of 100, the minimum optical receive power is -30 dBm for frequencies above three GHz.

In Figs. 17 and 18, we show the maximum optical power coupled into a detector for guided wave interconnect and broadcast interconnect. In these calculations, we assume that the transmitter emits one milliwatt of power and that the coupling efficiency into the guided wave distribution network is three dB. We further assume that the losses in the guided wave interconnect are minimal and that the number of ports is a variable. We also examine the case of a detector which subtends an area of 10^{-4} cm^2 and 10^{-2} cm^2 to evaluate the state-of-the-art of broadcast interconnect. The results of the Figs. 17 and 18 show clearly that broadcast interconnect is impractical for most systems applications unless a detector can be fabricated with an area of 10^{-2} cm^2. However, a detector as large as 10^{-2} cm^2 is a factor of ten larger than typical bonding pads in present day GaAs integrated circuits and thus will utilize a large fraction of the available integrated circuit area, unless it can be incorporated on the bottom of the chip. On the other hand, guided wave interconnect appears to be more than satisfactory for any reasonable number of ports up to the highest frequencies examined. We would thus conclude that the most likely interconnect scheme for GaAs integrated circuits would entail the use of guided wave interconnect.

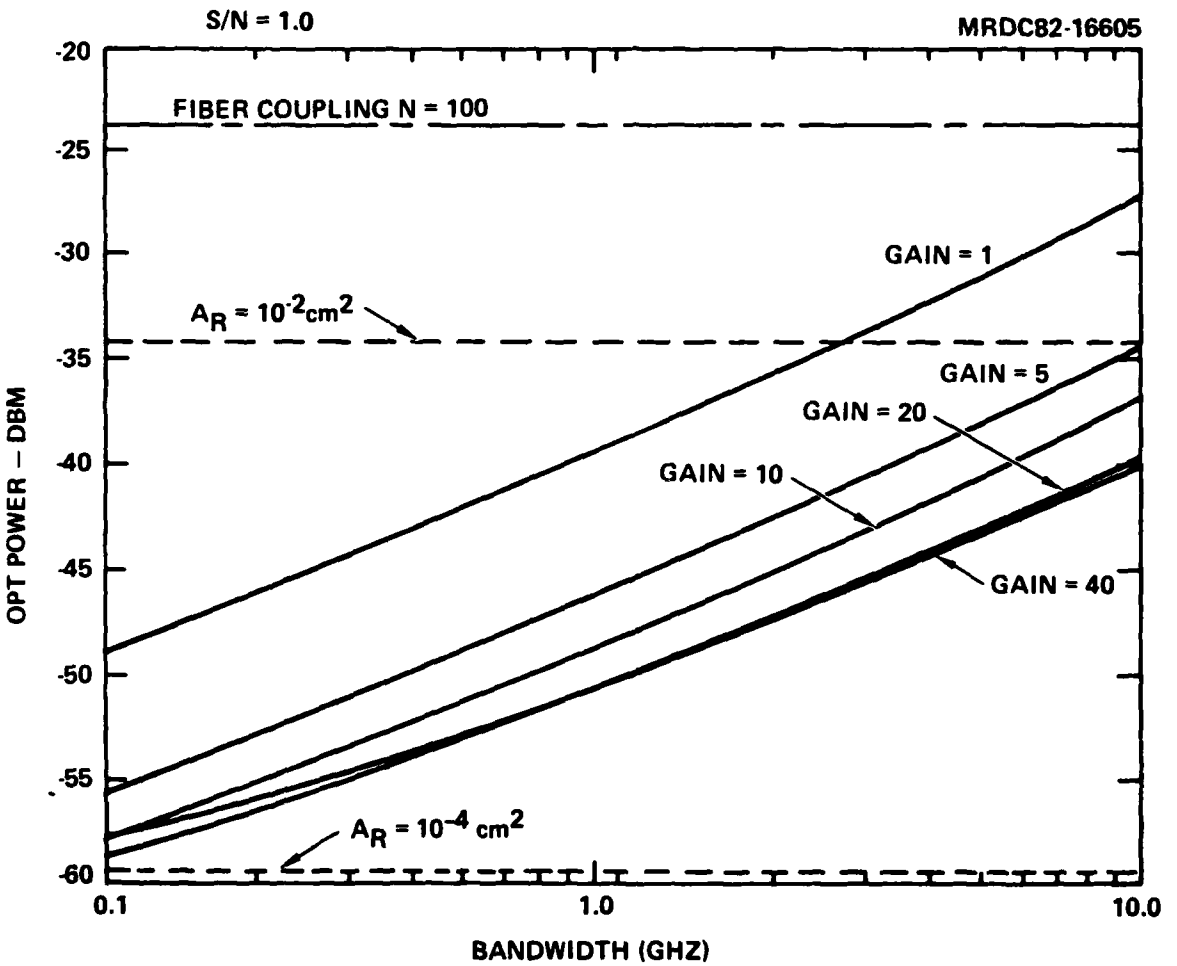
S/N = 1.0
MRDC82-16605
FIBER COUPLING N = 100
GAIN = 1
$A_R = 10^{-2} cm^2$
GAIN = 5
GAIN = 20
GAIN = 10
GAIN = 40
$A_R = 10^{-4} cm^2$
OPT POWER – DBM
-20
-25
-30
-35
-40
-45
-50
-55
-60
0.1
1.0
10.0
BANDWIDTH (GHZ)

Fig. 17

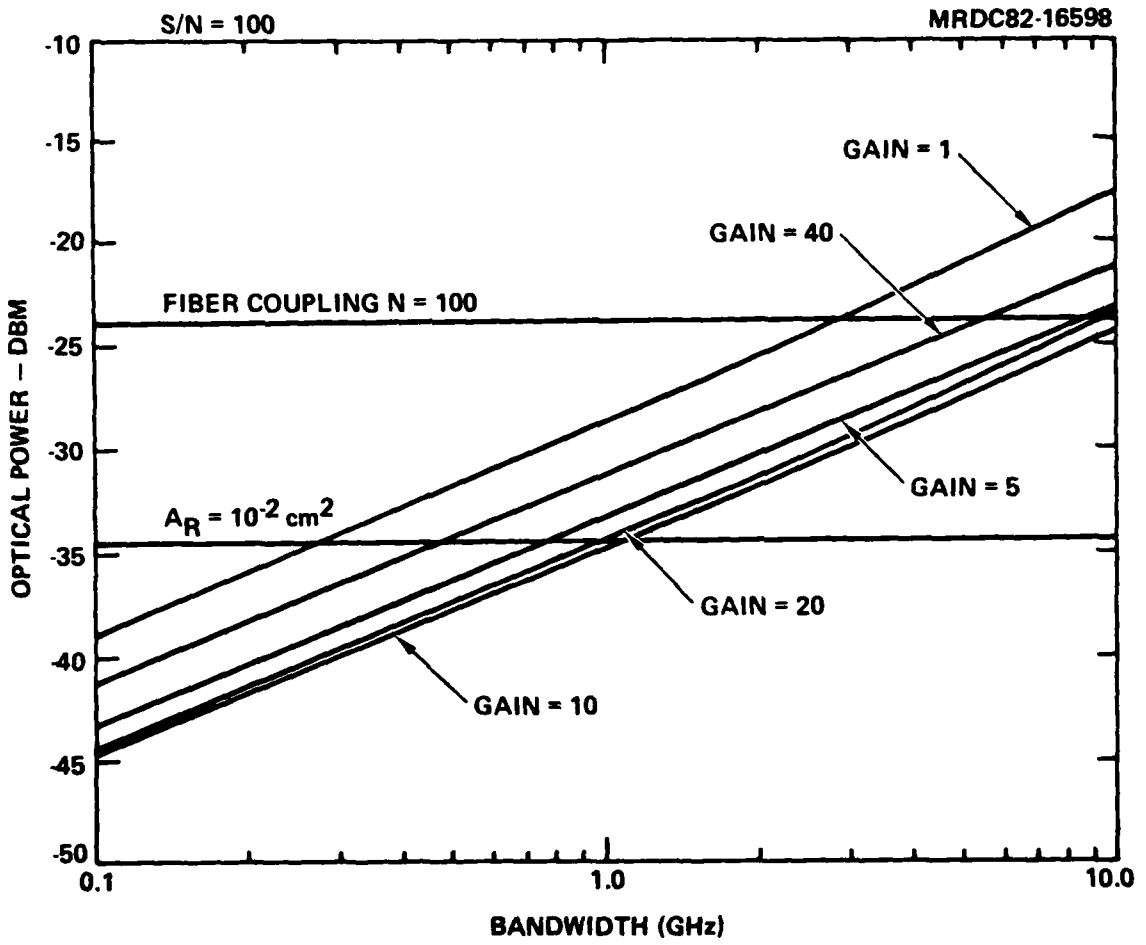
S/N = 100
MRDC82-16598
-10
-15
-20
-25
-30
-35
-40
-45
-50
GAIN = 1
GAIN = 40
FIBER COUPLING N = 100
GAIN = 5
$A_R = 10^{-2}$ cm^2
GAIN = 20
GAIN = 10
OPTICAL POWER – DBM
0.1
1.0
10.0
BANDWIDTH (GHz)

Fig. 18

4.0 INTEGRATED TRANSMITTER AND RECEIVER DESIGNS

Several factors must be considered in the design of an integrated transmitter/receiver port to be monolithically integrated with a GaAs integrated circuit. For the transmitter, these include threshold current, output power, heat sinking and optical coupling. For the receiver, they are signal-to-noise ratio, sensitivity and optical coupling. In the previous section, we have investigated three generic techniques for optical coupling of integrated circuits. At the data rates considered most reasonable for GaAs integrated circuits, only guided wave interconnect is feasible for long distances. Broadcast interconnect appears to be suitable for interconnection of ports on a single chip.

4.1 Laser Structure Design

The two primary considerations in the choice of a design for the laser structure to be used for a transmitter port are threshold current and optical coupling. Also of importance is the suitability of a particular structure for integration with integrated circuits. In this section, we considered two basic types of laser structures -- planar structures and epitaxial structures. Planar structures refer to laser designs which can be incorporated on the same surface of a wafer as integrated circuits. These structures are formed by processing subsequent to epitaxial growth of the lasers. Epitaxial structures are intended to include three dimensional structures grown by one or more epitaxial growths in which the light is guided parallel to the junction by a real index variation. The buried heterostructure is an example of an epitaxial structure. We will investigate geometrical factors in the fabrication of these devices and will determine from them the optimal size for a laser transmitter, based on known dependences of threshold current for the various structures.

Planar Structures

The three most widely used planar structures for the fabrication of double heterostructure lasers are the diffused stripe laser, the oxide or proton bombarded stripe laser, and the TJS laser. Of these structures, only the narrow diffused stripe laser[5] and the TJS laser[7] appear to be suitable for the low threshold requirements of an integrated transmitter. The TJS laser has the advantage that both contacts are easily accessible on the top surface of the device which makes it ideally suited for planar integration with integrated circuits. However, this laser appears to be very dependent upon the precise diffusion profile and doping level of the various layers to achieve the low thresholds which have been reported for it. The narrow diffused stripe laser is far less sensitive to growth parameters and diffusion profile but requires the extra processing steps necessary to make contact with n^+ contacting layer.

The TJS laser has been developed very successfully by workers at Mitsubishi[7] who have reported thresholds as low as 15 mA. The critical parameters in the structure are the length of the device, the width of the active region, and the near junction doping profile. The latter two are closely interrelated, as analysis shows that the low threshold operation of the TJS laser is very strongly dependent on the guiding of the light in the direction parallel to the epitaxial layers. As a result, the primary parameter that one can vary with the TJS is the length of the device. If we use the optimized values for layer thickness and doping profile reported in the literature, we find that the threshold current can be varied from 9 mA to 20 mA by varying the length of the device from 50 μm to 250 μm. 100 μm is considered the acceptable upper limit for the length of a device to be incorporated as a transmitter port on a complex IC.

The narrow diffused stripe laser shows relatively little dependence of the threshold current upon stripe width.[5] Figure 19 shows a set of L-I characteristics for 2, 4, and 8 μm stripe width NDS lasers fabricated at Rockwell. Note the small difference in threshold currents. This presumably

MRDC81-15469

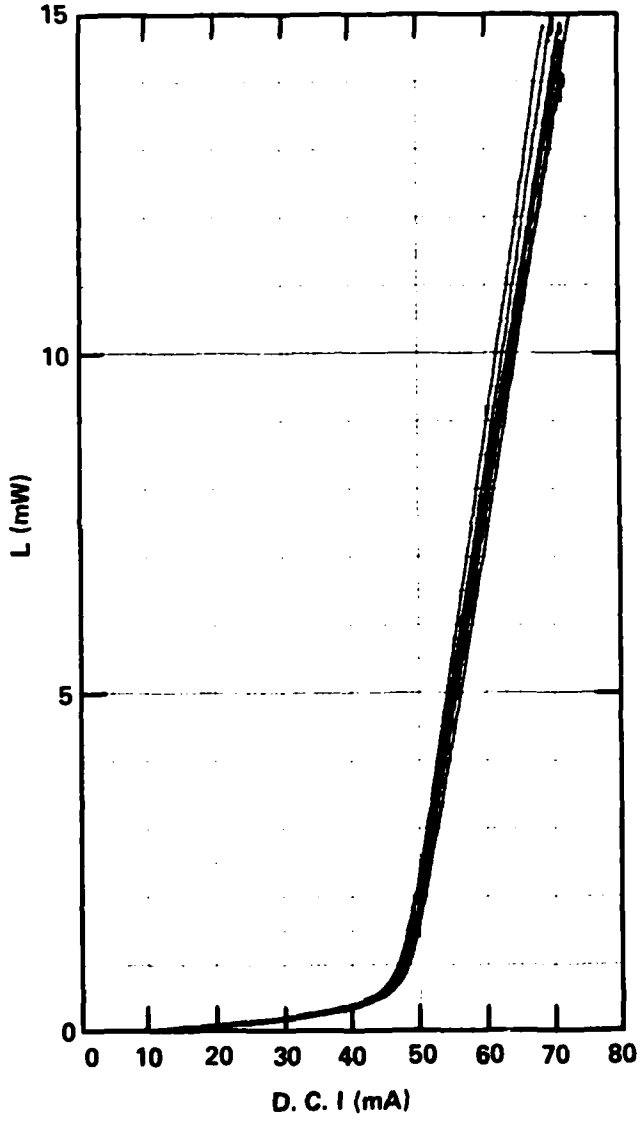

Fig. 19

results from spreading of the carrier distribution once the current is injected into the p-region near the active region of the device but may also result from the very weak guiding which occurs in this device. Also shown in that figure is the dependence of the laser threshold upon device length for a device with an optimized active layer thickness. Based on these data and a square root dependence of the threshold current on device length, we would anticipate that devices in the range of 50 μm to 100 μm long would have thresholds in the range of 13.5 mA to 19.0 mA (see Fig. 20).

Epitaxial Structures

The generic epitaxial structure to be considered here is the buried heterostructure. A variety of forms of this device structure have been fabricated which use advanced epitaxial technologies. For our purposes, we consider a device structure that is suitable not only for low threshold but is also suitable for incorporation into a grating feedback laser structure. The structure that we consider is shown in Fig. 21. This device utilizes a very thin active region with an asymmetrical cavity, so that the light generated in the active region spreads into the adjoining GaAlAs layer with lower Al composition. The majority of the optical wave travels in the GaAlAs waveguide and suffers little attenuation. At the same time, the guiding induced by the overgrowth of epitaxial layers confines the light in the direction parallel to the junction, so that a well defined optical power distribution is emitted from the cavity. Several devices of this type have been reported in the literature. However, at the present time, few data exist on the optimization of these devices for incorporation into a transmitter. As a result, we extrapolate these data from other device structures and assume that it is valid for the case of a buried heterostructure. Chinone, et al,[15] first reported a buried heterostructure of this type with the laser threshold as low as 30 mA for a 5 μm wide stripe and 300 μm long. However, Yariv and coworkers[16] have reported an epitaxial buried heterostructure device with a threshold as low as 9 mA for a 2 μm wide stripe. Based on these data, we will assume that the laser threshold varies linearly with stripe width and as the

MRDC81-15466

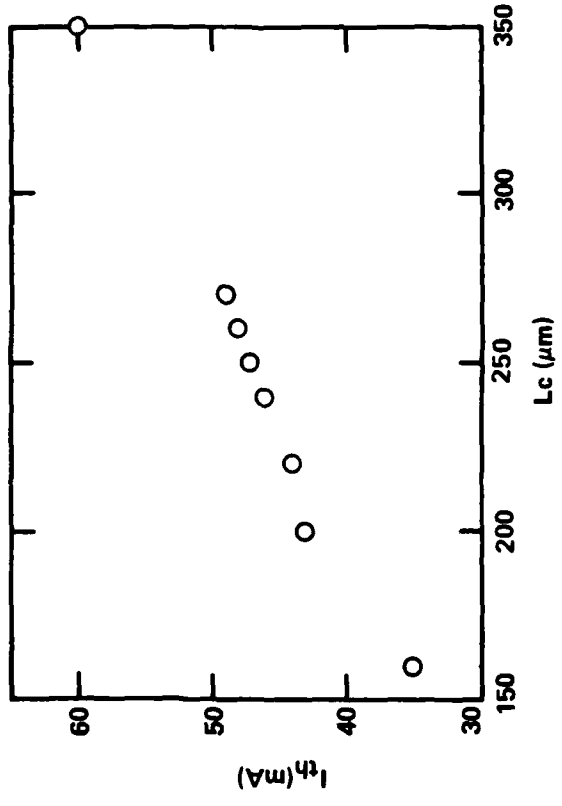

Fig. 20

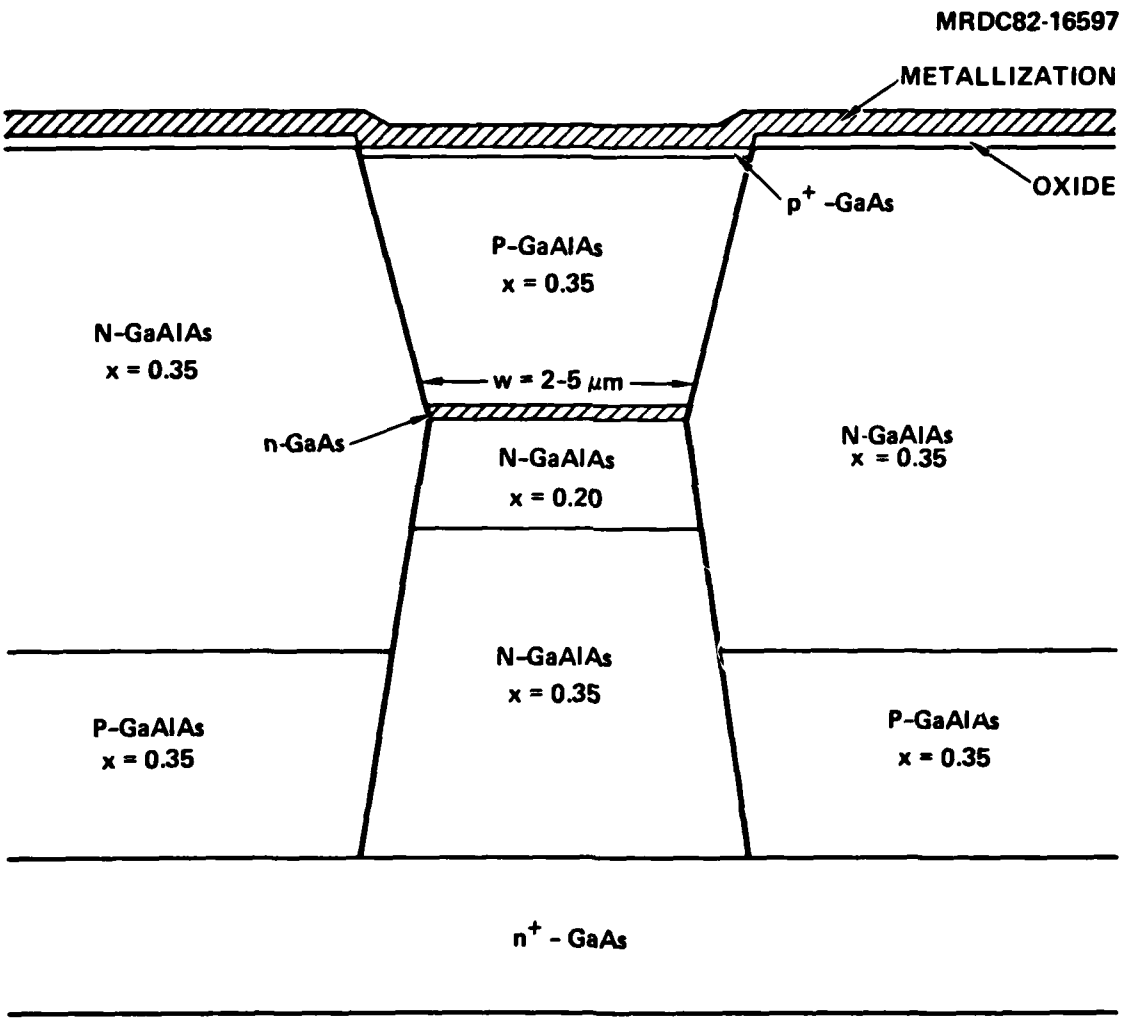
MRDC82-16597
METALLIZATION
OXIDE
p+ -GaAs
P-GaAlAs
x = 0.35
N-GaAlAs
x = 0.35
w = 2-5 μm
n-GaAs
N-GaAlAs
x = 0.20
N-GaAlAs
x = 0.35
N-GaAlAs
x = 0.35
P-GaAlAs
x = 0.35
P-GaAlAs
x = 0.35
n+ - GaAs

Fig. 21

square root of the length. Under these assumptions, it appears possible to fabricate a laser with a threshold current as low as three to four mA that utilizes a buried heterostructure design. This is clearly a much lower threshold than is achievable by any other design and illustrates the advantages of such a complex epitaxial structure. On the other hand, it is difficult to incorporate such a structure onto the top surface of an integrated circuit. The device requires at least two layers of epitaxial growth and requires relatively fine processing between the growth of the layers.

4.2 Mirror Fabrication Techniques

The incorporation of lasers into complex integrated circuitry will require the use of an optical feedback structure other than cleaved mirrors. Several alternatives to cleaved mirrors have been investigated. The two approaches which seem to provide the most promise for large scale integrated circuit processing are the etched mirror laser and the distributed feedback laser. The etched mirror is essentially a Fabry-Perot mirror laser in which the mirrors are formed by chemical or dry etching processes rather than cleaving. Included in this category is a recently described micro-cleaved mirror in which cantilever sections of lasers are formed and then cleaved by ultrasonic agitation to form cleaved mirrors on the wafer.[41]

A number of studies on the etching of semiconductor laser mirrors has been performed. For the purposes of this report, it is important to note that in general these device structures closely approach the performance of cleaved mirror lasers. For example, Table I shows the performance achieved for a variety of etched mirror approaches in the GaInAsP system as well as in the GaInP system. On the basis of this work, we would conclude that etched mirrors are capable of yielding laser thresholds within 20 to 30% of the etched mirror values. The primary cause of this difference is nonplanarity of the laser mirrors due to preferential chemical etching and roughness of the mirror surface due to nonuniform etching. These two factors contribute approximately equally to increase in threshold observed for chemically and dry

etched mirrors. With the chemically etched mirror, it should be possible to fabricate lasers of essentially any length, from 50 μm up to any standard value.

Table I

Comparison of Etched Mirror Lasers

Material/Technique	$J_{th}^{(etched)}/J_{th}^{(cleave)}$	$\eta_{diff}^{etched}/\eta_{diff}^{cleaved}$	Ref.
GaAlAs/GaAs Wet Chemical Etching	1.3-1.5	0.25	42
GaInAsP/InP Wet Chemical Etching	1.3-1.5	0.66	43
	1.1	0.80	44
GaInAsP/InP Reactive Ion Etching	1.1-2.0	0.80	45

The second alternative to a cleaved mirror laser is generically referred to as the distributed feedback laser.[46-57] Two examples of a distributed feedback laser are shown in Fig. 22. Here, the optical feedback is provided by a grating that is incorporated into the optical cavity of the device. To understand the operation of a grating in a semiconductor laser, consider part b of Fig. 22. Here we show the propagation of an optical wave through a waveguide containing a corregated interface. Assume that the scale of the corregations is appropriate for high efficiency feedback of the optical wave. At each corregation, some small fraction of the wave is reflected due to the nonplanarity of the interface and effective spatical variation of the refractive index. If the period of these reflections is appropriate, the reflected waves constructively interfere and add in phase and propagate in the opposite direction. This physical argument accounts for Eq. (22) which specified the phase matching condition.[46]

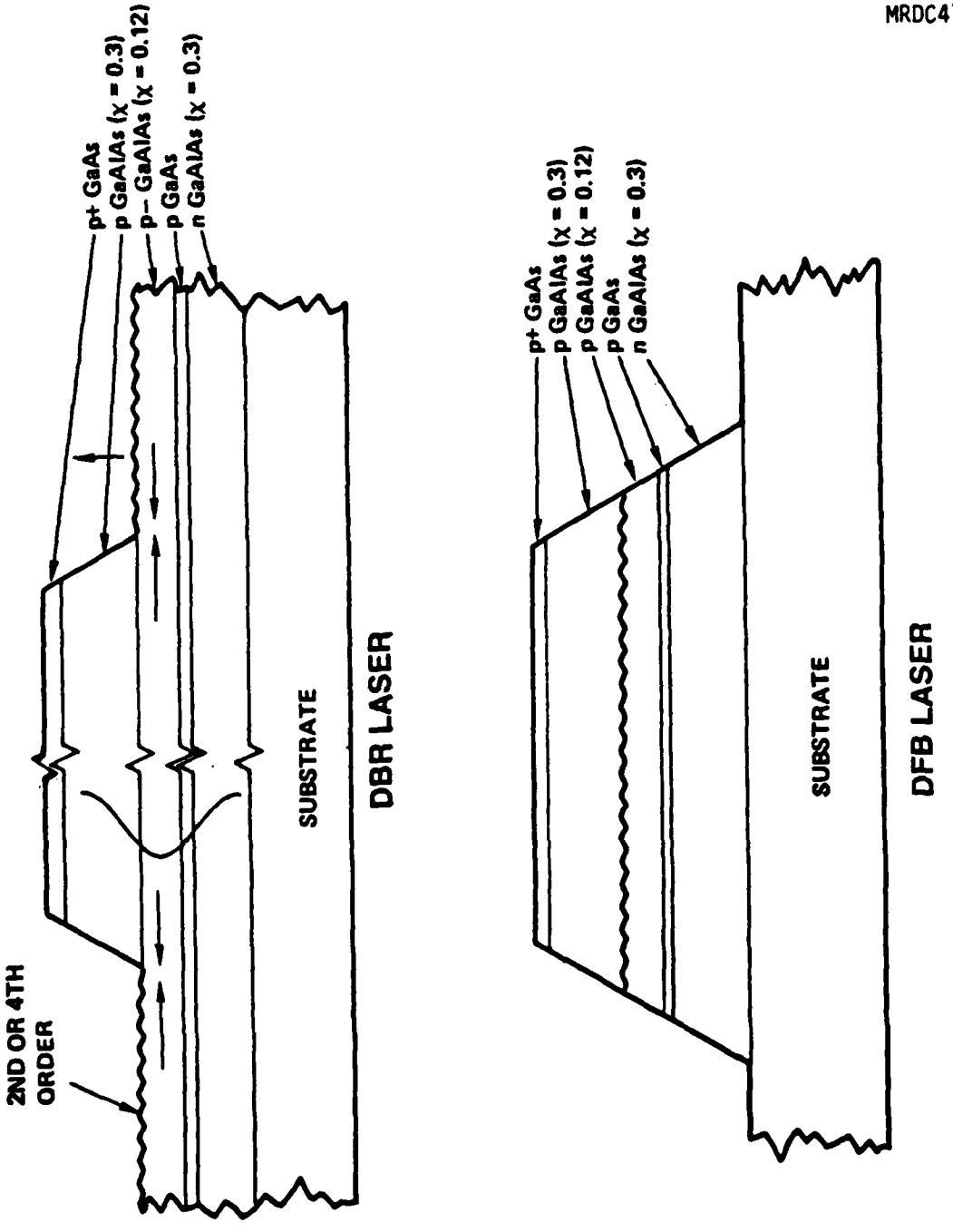
p+ GaAs
p GaAlAs (χ = 0.3)
p– GaAlAs (χ = 0.12)
p GaAs
n GaAlAs (χ = 0.3)
SUBSTRATE
DBR LASER
2ND OR 4TH ORDER
p+ GaAs
p GaAlAs (χ = 0.3)
p GaAlAs (χ = 0.12)
p GaAs
n GaAlAs (χ = 0.3)
SUBSTRATE
DFB LASER

Fig. 22

$$\Lambda = \frac{\lambda_b}{2\bar{n}} \tag{22}$$

where Λ is the grating period, λ_b is the free space wavelength, and $\bar{n}$ is the average index of refraction. The usual analysis to describe the behavior of a distributed feedback device uses a coupled mode analysis and considers the coupling between a backward and forward propagating electromagnetic wave due to the presence of a periodic variation of the refractive index. The relevant parameters that are determined from this analysis are the feedback coupling coefficient, κ, which is a measure of the fractional reflection of the propagating wave due to the periodic index variation, and the loss coefficient, α, due to refraction of waves out of the cavity. These quantities are determined for a periodic variation of the index as shown in Fig. 23. The analytical expression for the coupling coefficient is given in the following equation:[46]

$$K^{\ell} = k_0 C_{-\ell}(n_3 - n_1)\,\Omega \tag{23}$$

The parameters shown in this equation are defined as follows. k_0 is the undisturbed propagation constant of the radiation in waveguide. $C_{-\ell}$ is the Fourier coefficient of the ℓ^{th} order Fourier component of the refractive index variation, and Ω is the fraction of the unperturbed field that is contained in the corregated portion of the waveguide. This expression must be evaluated for a particular waveguide configuration and spatial dependence of the index of refraction. The coupling constant for first, second, and third order gratings are calculated for the waveguide shown in Fig. 23. The active region of the guide is chosen 1 μm thick because the laser design will be of a large optical cavity design in which the majority of the radiation is propagating in a passive GaAlAs waveguide region. As can be seen from this figure, there is large difference in the distributed feedback coupling constant at a given grating height between the first, second, and third order gratings. In addition to reflecting the radiation less efficiently than the first order grating, higher order gratings also radiate light from the guide owing to lower order Bragg scattering. The angle at which radiation is emitted is given by[47]

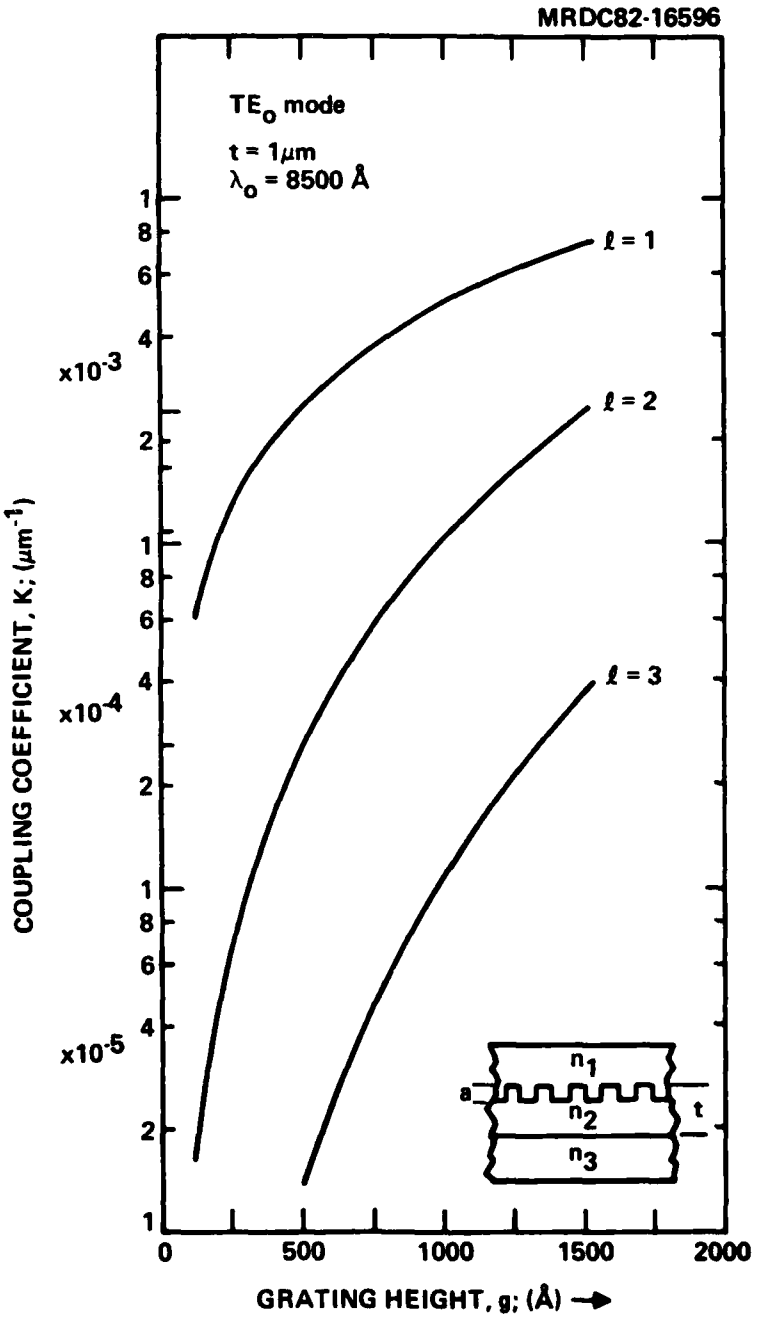
MRDC82-16596
TE$_o$ mode
t = 1μm
λ$_o$ = 8500 Å
ℓ = 1
ℓ = 2
ℓ = 3
x10^{-3}
x10^{-4}
x10^{-5}
COUPLING COEFFICIENT, K; (μm^{-1})
GRATING HEIGHT, g; (Å) →
0
500
1000
1500
2000
n$_1$
n$_2$
n$_3$
a
t

Fig. 23

$$\sin \theta = 2 (m/\ell) - 1 \tag{24}$$

where ℓ is the order of the grating and m is an integer that can assume any value from 0 to ℓ. The possible scattering angles for a first, second, and third order grating are shown in Table II.

Table II

Order	Scattering Angles
1	0, 180
2	0, 90, 180
3	0, 70, 110, 180

Even order gratings can scatter light perpendicular to the wave guide plane.

The radiation loss constant for first order Bragg scattering can be calculated for the grating of Fig. 23 from[48]

$$\alpha = \frac{(ka)^2}{2W_{eff}\, n_m} (n_1^2 - n_m^2)(n_1 - n_2) \tag{25}$$

This is shown in Fig. 24 for a second order grating. Note that for a grating period of 2450 Å, the Bragg period, the loss coefficient is 3.6 cm^{-1}.

Bragg reflection and scattering can be used to feed back and couple radiation from a DFB or DBR laser. The reflectivity of a grating section of length L can be calculated from

$$R = \left| \frac{\kappa \sinh [(\kappa^2 + \alpha^2)^{1/2} L]}{\alpha \sinh[(\kappa^2 + \alpha^2)^{1/2} L] + (\kappa^2 + \alpha^2)^{1/2} \cosh[(\kappa^2 + \alpha^2)^{1/2} L]} \right|^2 \tag{26}$$

for a first order grating $\alpha = 0$. For a second order grating, $\alpha = 3.6$ cm^{-1} for a 1000 Å deep grating at the Bragg period.

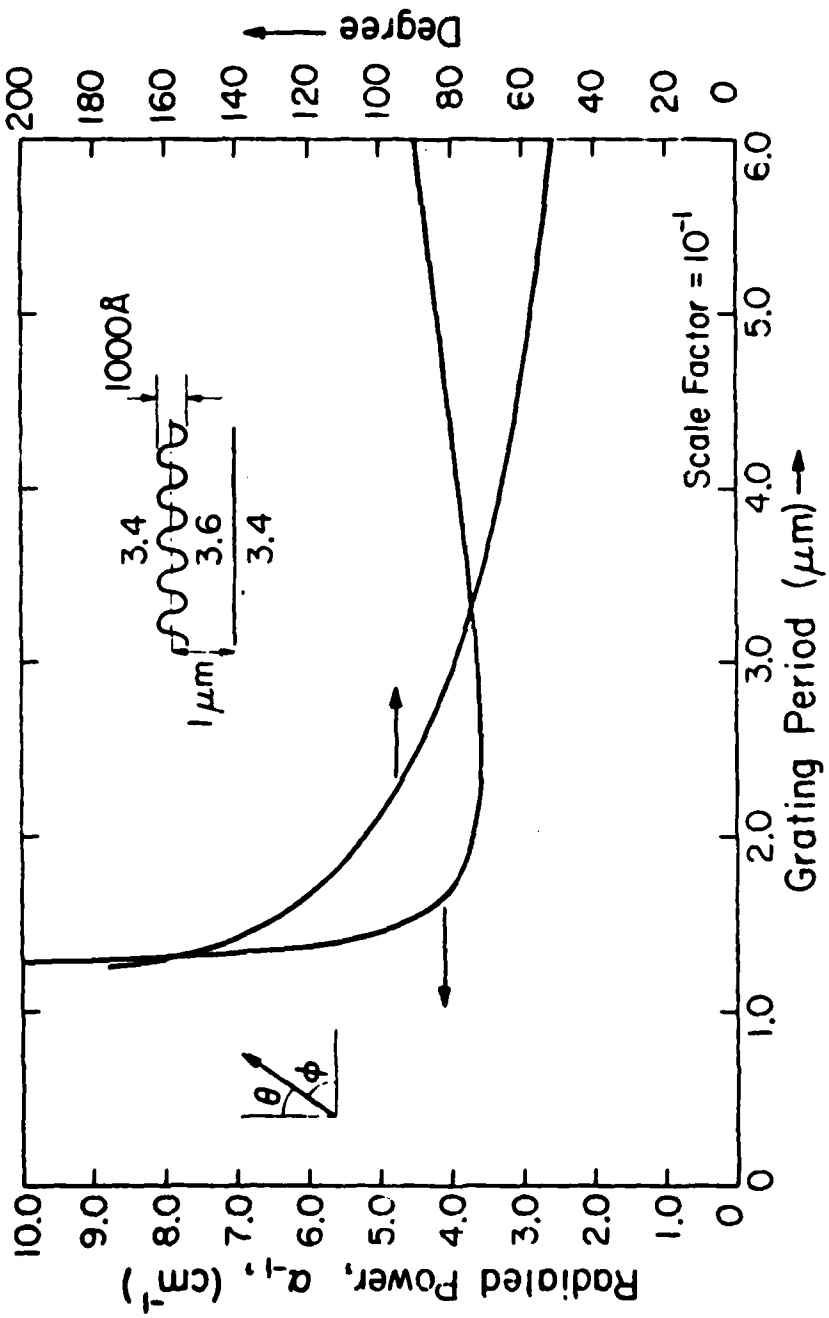
Degree
200
180
160
140
120
100
80
60
40
20
0
6.0
5.0
4.0
3.0
2.0
1.0
0
Scale Factor = 10^{-1}
Grating Period (μm) →
Radiated Power, α_{-1}, (cm^{-1})
10.0
9.0
8.0
7.0
6.0
5.0
4.0
3.0
2.0
1.0
0
1000Å
3.4
3.6
3.4
1μm
θ
ϕ

Fig. 24

The importance of this difference in the design of a laser for use in an integrated circuit is demonstrated in the reflectivity of a passive grating reflector of the type used in a DBR laser. This is illustrated in Fig. 25, where we show the dependence of the length of grating necessary to achieve 50% of the maximum reflectivity for first and second order gratings. The calculation for the second order grating include the effect of first order radiation loss. This limits the maximum reflectivity of the second order grating to ≈ 50%. To achieve a reflectivity of 50% in a practical size grating (<50 μm), it will be necessary to use a first order grating. A second order grating can only be used in the case where coupling of the radiation perpendicular to the plane of the laser is required. Two things are apparent from this figure. First, the first order grating is considerably more efficient as a reflector than the second order grating at a given grating depth. This is demonstrated by the shorter grating length necessary to achieve a certain reflectivity. Second, the grating depth for either grating must be comparable to the period for a reflector with length less than 400 μm to be constructed. To achieve a reflectivity of 50% in a practical size grating (<50 μm), it will be necessary to use a first order grating. A second order grating can only be used in cases where coupling of the radiation perpendicular to the plane of the laser is required.

The use of a distributed feedback structure alters the threshold condition for a laser. In a DBR, the facet reflectivity is replaced grating reflectivity per Eq. (26). The threshold condition for a DFB laser must take into account the distributed nature of the feedback mechanism and any loss from radiation by the grating. The threshold conditions for a distributed feedback laser are described below.[53]

$$\frac{\exp[\Gamma(g_{th} - G_{th} - \alpha_{fc})L]}{\Gamma^2(g_{th} - G_{th} - \alpha_{fc})^2 + 4\,\delta_q^2} = \frac{1}{(\kappa^{\ell})^2} \qquad (27)$$

$$\delta_q L = (q - 1/2)\pi$$

Fig. 25a

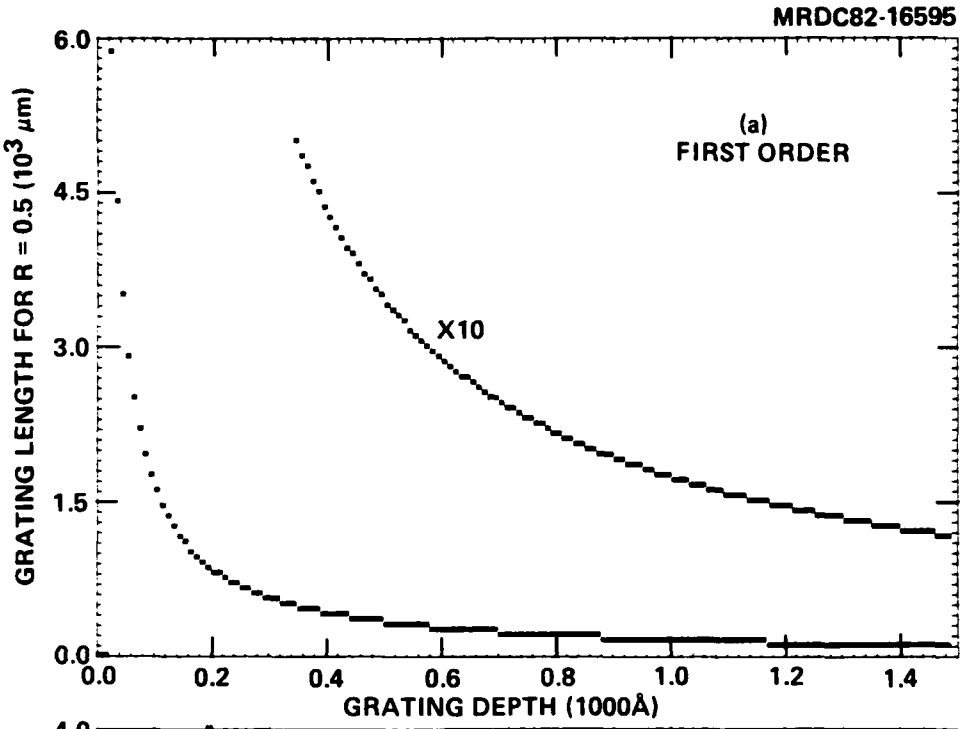

Fig. 25b

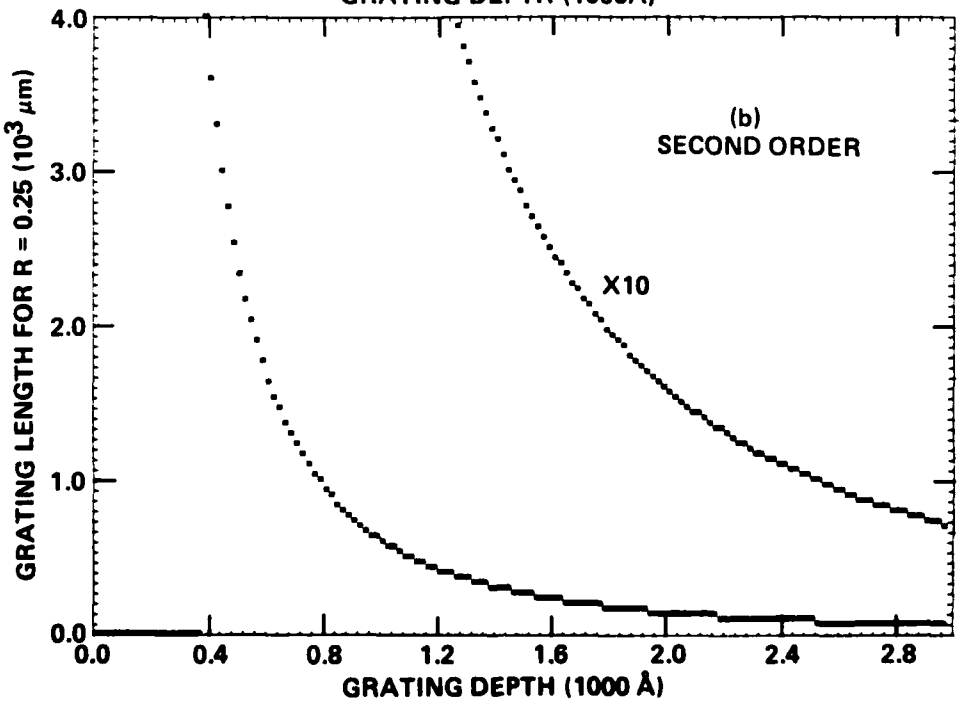

g_{th} is the gain at threshold, G_{th} is the gain needed to overcome losses external to the active region, α_{FC} is the loss in the active region, and Γ is the mode confinement factor. Since the reflectivity is a distributed parameter, it is coupled with the distributed losses to describe the gain in threshold condition. Note that this assumes an infinitely long laser structure or a laser with perfect antireflection coatings on the surface of the device. To achieve low threshold operation of a distributed feedback laser, it will be necessary to fabricate very high aspect ratio gratings in either the first or second order. This requires then that gratings with periods that range from 1700 to 2450 Å must be fabricated which have depths in excess of 500 Å. At present, this is a difficult task to achieve. However, in view of the potential of DFB lasers to allow perpendicular coupling of the light from the laser, the benefits for coupling light into waveguides and other optical cavities is great, and as a result the DFB laser is a viable device.

4.3 Light Coupling

The crucial aspect of the transmitter for application to an interconnect scheme is the coupling of the light into the optical distribution system. The present study has indicated that it will be required to use either etched mirror or distributed feedback lasers to enable the fabrication of the lasers on any portion of an IC wafer. For coupling into either a guided wave optical distribution system or broadcast distribution system, it should be possible to accommodate either an edge coupled geometry or a perpendicular coupled geometry. The Fabry-Perot laser is most suitable for edge coupling, since the light is emitted in a direction parallel to the junction plane, and the feedback plane is perpendicular to this direction of plane. On the other hand, the distributed feedback and distributed Bragg laser are suitable for perpendicular coupling or edge coupling geometry.

The edge coupling possibility is most interesting because of the availability of an accurate alignment technology for fibers using preferentially etched groves in Si substrates. This allows accurate aligment of the fibers to the lasers or detectors on the edge of the substrate. Coupling has the disadvantage of removing transmitter and receiver positioning

flexibility when the lasers and detectors are mounted on the top surface of the I.C. chip. As a result, edge coupling is best implemented if the transmitters and receivers are mounted on the bottom side of the chip as shown in Fig. 26. To accomplish this will require the development of an electrical via technology that allows high resolution deep vias to be fabricated in GaAsIC wafers. Potential methods for forming these vias are laser drilling[58] and reactive ion etching. Backside processing has the following advantages:

1) It allows optimized processing for the electronic and optical devices.

2) It improves the heatsinking of the optical devices

3) It reduces optical-electronic device interaction

4) It promotes higher yield in that redundancy can be built into the optical devices.

These advantages make backside processing attractive regardless of the coupling scheme.

4.4 Transmitter Drive Design

A high data rate driver for the GaAlAs/GaAs laser can be designed around GaAs FET and TELD. Figure 27 illustrates three simple drivers for a low threshold GaAs laser. Figure 27a shows a TELD connected in series with the laser. When the gate of the TELD is pulsed, the driver moves from the quiescent operating point (1) to operating point (2). The laser which is biased above threshold at (1) is turned off by this change in bias point. Thus, the laser produces a zero pulse for a negative going gate pulse. The duration of the pulse is the transit time of the Gunn domain in the device. The transmitter in Fig. 27b and Fig. 27c can be operated in either a positive or negative logic configuration depending on whether the drive FET is a

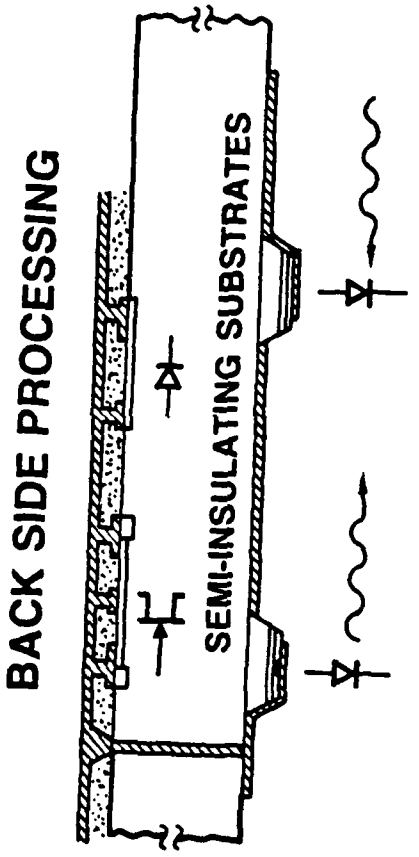

Fig. 26

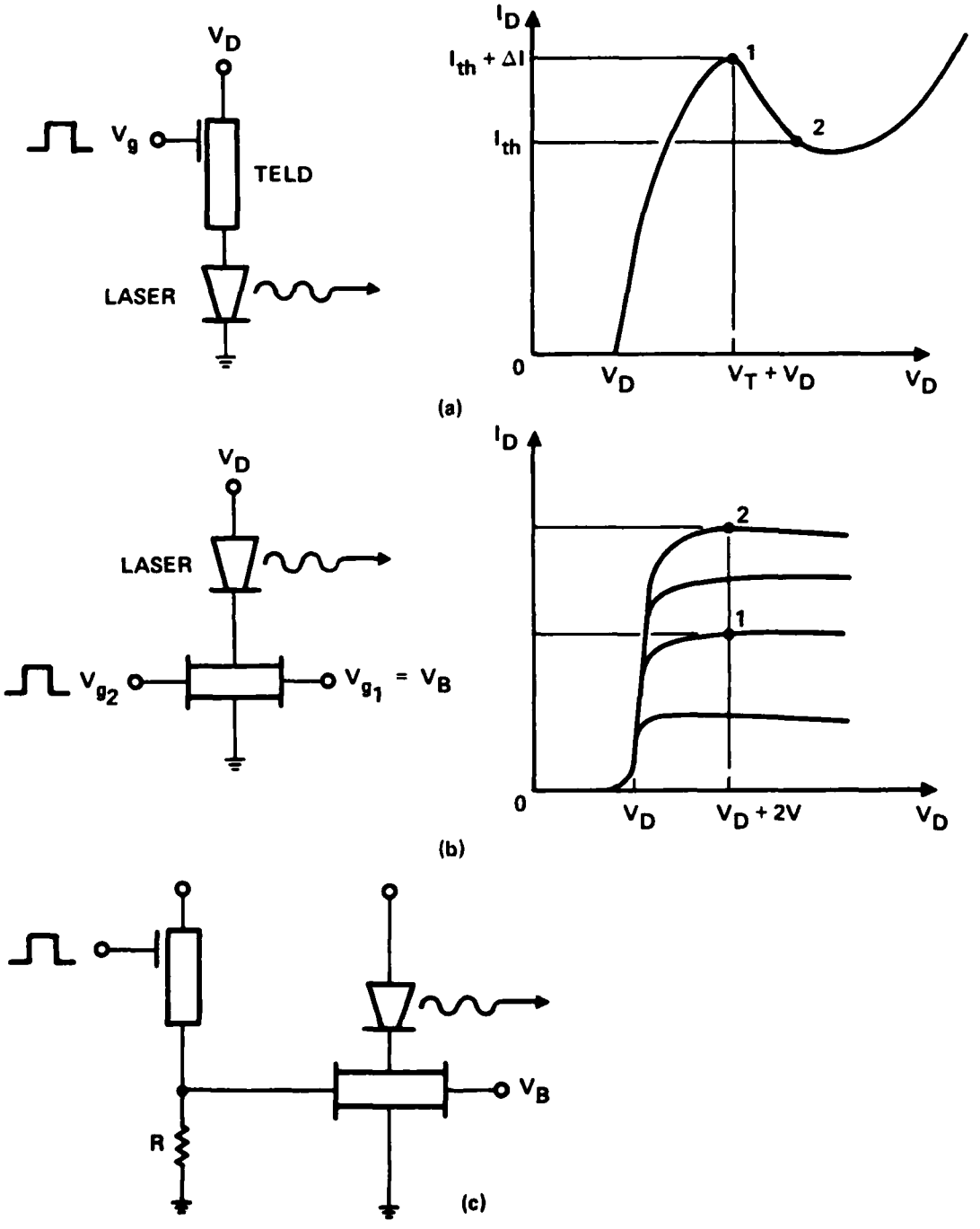
V_D
V_g
TELD
LASER
I_D
$I_{th} + \Delta I$
I_{th}
1
2
0
V_D
$V_T + V_D$
V_D
(a)
V_D
LASER
V_{g_2}
$V_{g_1} = V_B$
I_D
2
1
0
V_D
$V_D + 2V$
V_D
(b)
V_B
R
(c)

Fig. 27

depletion mode device or an enhancement mode device. The logic pulse is applied directly to the FET gate, and no discrimination is used. In Fig. 27c, the pulse must be enough to trigger a domain in the TELD.

The design of the elements for these transmitters depends upon the characteristics of the laser. Based on the analysis of Section 4.1, we assume an optimized laser with the following characteristics:

$$I_{th} = 5 \text{ mA}$$

$$\eta_{diff} = 30\%/\text{facet}$$

The operating power is one mW. Thus, the modulation current is two to three mA.

TELD Transmitter

The design of the TELD (shown in Fig. 28) is determined by the laser characteristics and the properties of Gunn devices.

The anode-to-cathode separation for the TELD is determined by the desired duration for the current pulses. For a transmitter designed for operation at a bit rate B, the current pulse duration τ_p should satisfy

$$\tau_p < 1/B \quad . \tag{28}$$

In this example, we chose B = 4 Gb/s, so $\tau_p < 250$ ps. To provide 50 ps margins for turn on and turn off of the TELD, the design assumes a value of $\tau_p \sim 150$ ps. Since

$$d \sim 10^7 \tau_p \text{ (cm)} \quad , \tag{29}$$

with τ_p in seconds, then in this case d = 15 μm. The threshold voltage can be calculated from

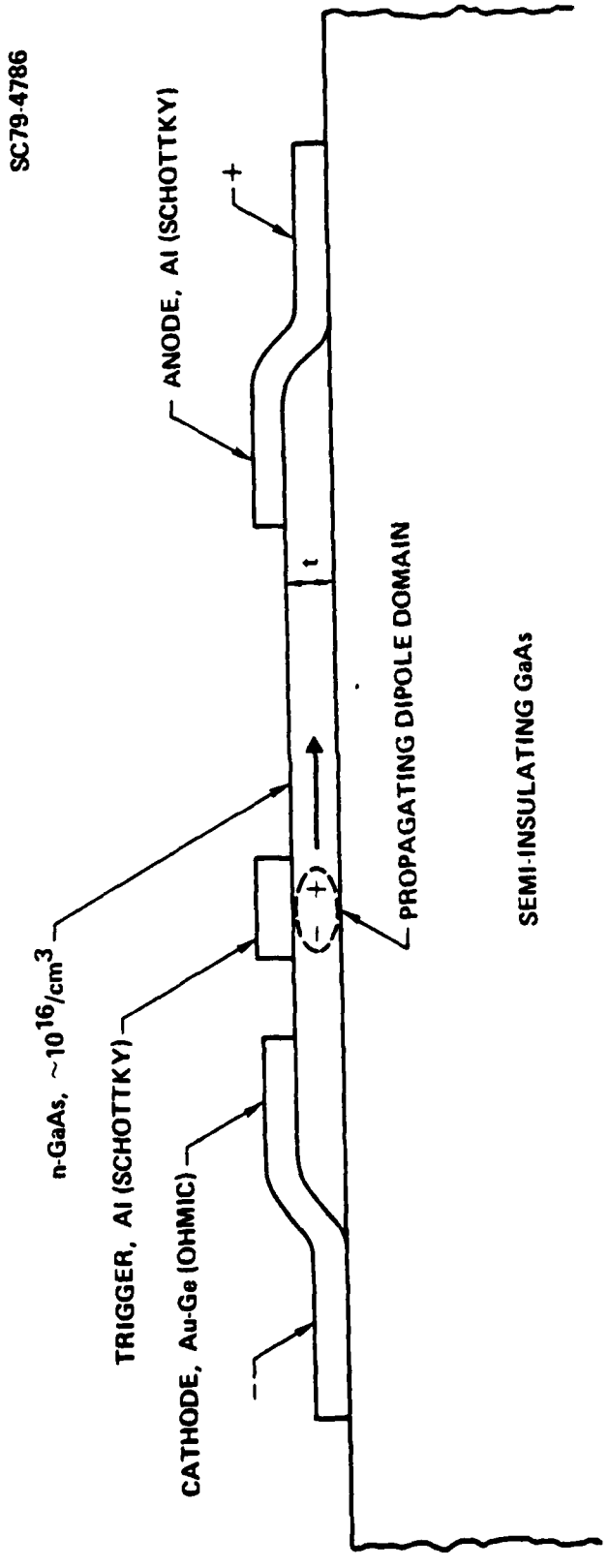
SC79-4786
ANODE, Al (SCHOTTKY)
+
t
PROPAGATING DIPOLE DOMAIN
SEMI-INSULATING GaAs
n-GaAs, ~10^16/cm^3
TRIGGER, Al (SCHOTTKY)
CATHODE, Au-Ge (OHMIC)
-

Fig. 28

$$V_t = E_t d \quad , \tag{30}$$

where E_t is the threshold electric field. With E_t = 3300 V/cm in GaAs then V_t = 5 volts in the case considered.

The doping level and dimensions of the active region affect the formation and stability of dipole domains and determine amplitude of the current pulses as well as the average (dc) power dissipation. It has been determined from studies of planar TELD oscillators that, to ensure full domain formation and propagation, the product of carrier concentration n and length d of the active region should satisfy the relation.

$$nd > 10^{13}\ cm^{-2} \tag{31}$$

while the product of n and the thickness t of the active layer should satisfy

$$nt > 10^{12}\ cm^{-2} \tag{32}$$

The influence of the dimension of the active layer on the series resistance R_S of the device is given by the relation

$$R_S = \frac{L}{e\mu nwt} \tag{33}$$

when e is the electronic charge (= 1.6×10^{-19} C), μ is the carrier mobility, t is the layer thickness, and w is the channel width. The dc current for bias near the threshold is then given by

$$I_t = \frac{e\mu ntwV_t}{d} = e\mu ntwE_t \quad . \tag{34}$$

Substituting numerical values into this equation, E_t = 3300 V/cm for gallium arsenide and $\mu \sim 6700\ cm^2/V\text{-}s$ (typical for high-quality epitaxial layers in gallium arsenide) gives

$$I_t = 3.5 \times 10^{-12}\ ntw \quad . \tag{35}$$

Using the design values of

$$n = 2 \times 10^{16}/cm^3$$

$$t = 1 \times 10^{-4} \text{ cm}$$

$$\omega = 10 \ \mu m$$

it follows from the preceding equation that

$$I_t = 7 \text{ mA} \quad .$$

Assuming a 50% drop in current when a domain is produced, the change in current is

$$\Delta I_{TELD} = 0.5 \ I_t = 3.5 \text{ mA} \quad . \tag{36}$$

Note that in this example

$$nd = 3 \times 10^{13} \text{ cm}^{-2}$$

$$nt = 2 \times 10^{13} \text{ cm}^{-2} \quad .$$

The choice of electrode materials is dictated by the desire to obtain stable operation under dc-biased conditions. The normal procedure would be to use ohmic electrodes for both anode and cathode, but experience with TELD devices has shown that better dc-bias performance is obtained with a Schottky barrier anode, due to hole injection at the anode. Thus, it is expected that best performance for the photodetector will be obtained with an ohmic contact, such as Au-Ge, at the cathode and a Schottky barrier contact, such as Al, for the anode and trigger electrodes.

With these design parameters, the area taken by the TELD Transmitter is approximately

$$A_T = A_L + A_D + A_i \tag{37}$$

where A_L is the laser area, A_D is the driver area, and A_i is the area necessary for metallization. If we wish A_T to be less than 10^{-4} cm^{-2}, A_D = 10 μm x 2.5 μm = 2.5 x 10^{-6} cm^2, and A_L = 50 μm x 20 μm = 10^{-5} cm^2, A_i can be as large as 8 x 10^{-5} cm^2. Clearly, a compact transmitter can be fabricated using the design criterion above.

FET Transmitter

The FET is also a three-terminal device, but unlike the TELD it has a dependence of output current on input voltage which is approximately linear over a fairly wide operating range. The three terminals are designated source, gate, and drain, as indicated in Fig. 29. In gallium arsenide, the electrodes are fabricated on a thin n-type layer, with ohmic contacts for source and drain and a Schottky barrier for the gate. When a bias voltage is applied between source and drain, a current flows through the n-type layer. The source-to-gate bias controls the source-to-drain current by regulating the thickness of the depletion layer under the Schottky gate electrode. No current flows in the depletion layer, so that increasing the negative gate bias decreases the drain current. The current is completely shut off for a negative gate voltage large enough to completely deplete the layer under the gate. This voltage is known as the "pinch off" voltage, V_{po}. For zero applied gate voltage, the region under the gate is partially depleted due to the Schottky barrier potential. The "built in" potential responsible for the depletion, V_{bi}, equals -0.8 V in GaAs. This depletion region disappears for a positive gate voltage of 0.8 V, in which case the source-to-drain current reaches its maximum, or saturated, level I_{sat}. This important parameter of the GaAs FET is given by

$$I_{sat} = nev_s wt \quad , \tag{38}$$

where n is the carrier concentration in the active layer, e is the electronic charge, v_s is the electron saturation velocity, w is the gate width, and t is

SC79-4788

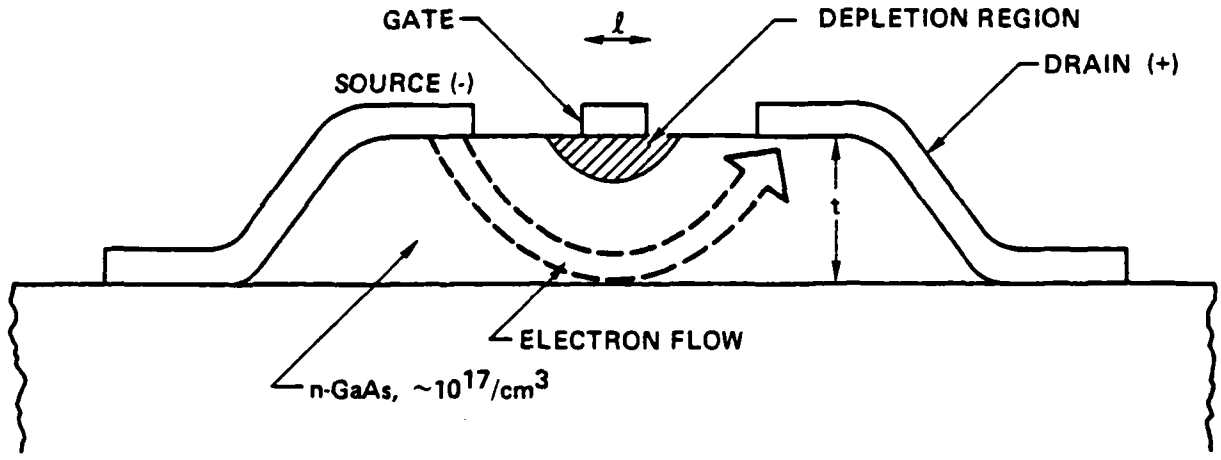

Fig. 29

the active layer thickness. The drain current is given in terms of the applied voltage by

$$I_d = I_{sat}\left[1 - \left(\frac{V_{gs} + V_{bi}}{V_{po} + V_{bi}}\right)^{1/2}\right] \quad , \tag{39}$$

with V_{po} given by

$$V_{po} = \frac{-net^2}{2\varepsilon} + |V_{bi}| \quad , \tag{40}$$

where ε is the dielectric constant of the material. The transconductance g_m is given by

$$g_m = \frac{\partial I_d}{\partial V_{gs}} = -\frac{1}{2} I_{sat}[(V_{gs} + V_{bi})(V_{po} + V_{bi})]^{-1/2} \quad . \tag{41}$$

Another very important parameter is the input capacitance C_{gs}, given by

$$C_{gs} = \frac{\frac{1}{4}(2ne\varepsilon)^{1/2}\, \ell\, w}{(V_{gs} + V_{bi})^{1/2}} \quad , \tag{42}$$

where ℓ is the gate length. This capacitance determine how large the input impedance to the FET can be, consistent with a given bandwidth.

In designing the FET for high-speed operation, it is desirable to maximize the transconductance-to-capacitance ratio. In fact, it can be shown that

$$g_m/C_{gs} \approx V_{sat}/\ell \quad . \tag{43}$$

Thus, the gate length ℓ should be as small as possible. We chose $\ell = 0.8$ μm, a value consistent with present photolithography capability in our laboratory. The active layer thickness should be considerably less than the gate length to assure uniform pinch-off; we choose $t = 0.20$ μm. Other parameters consistent with present low power FET design and fabrication capability are $n = 1.5$ x

$10^{17}/cm^3$ and W = 50 μm. From Eq. (3), using the value $v_s = 0.8 \times 10^7$ cm/s appropriate for GaAs, it follows that

$$I_{sat} = 19.2 \text{ mA}$$

and, with $\varepsilon = 9.7 \times 10^{-13}$ f/cm for GaAs,

$$V_{po} = -4.9 \text{ volts}$$

A variation in V_{gs} from -3.4 V to -2.8 V gives a change in I_d from 5.0 mA to 7.0 mA, or ΔI_d = 2 mA. This should be adequate to drive our injection laser diode at high modulation speeds. Values of the capacitance C_{gs} for these two values of V_{gs} are ≈ 0.02 pf and ≈ 0.12 pf, respectively.

The area of our transmitters in the case above is give by

$$A_T = A_D + A_L + A_i \tag{44}$$

The area of the driver is twice the area of the FET. A_D = 2 x 50 μm x 15 μm = 1.5×10^{-5} cm^2. Thus, the area available for interconnect or FET expansion is 7×10^{-5} cm^2.

TELD-FET Transmitter

The combination transmitter of Fig. 27c has the advantage of providing the appropriate pulse shape to drive the FET laser. The TELD must be redesigned to accommodate the FET drive. If the response time of the FET is to be kept much less than 250 ps, then

$$t_o = R_1 C_{gs} \ll 250 \text{ ps} \approx 25 \text{ ps} \tag{45}$$

for C_{gs} = 0.12 pf $R_1 \cong 200\ \Omega$.

The current drop in the TELD must be large enough to modulate the FET

$$\Delta I \; R_1 = \Delta V_{gs} \tag{46}$$

$$\Delta I = 0.5 \; I_t = \frac{\Delta V_{gs}}{R_1} = \frac{1.5 \text{ V}}{200 \; \Omega}$$

$$I_t = 15. \text{ mA}$$

$$\Delta I = 7.5 \text{ mA}$$

Thus, using the design criterion for the TELD, w = 21 μm, and the area of the driver is $A_D = 2 \; A_{FET} + A_{TELD} + A_{res}$. The resistor area is given by

$$R = \frac{\rho}{t} \frac{L}{w} \tag{47}$$

using the FET material for the resistor $\rho/t = 10^3 \; \Omega/\square$; thus L/w = 0.2. If w = 50 μm, L = 10 μm and R_{res} = 50 μm (10 + 10) μm = 10^{-5} cm^2. The area of the TELD is now 25 μm x 21 μm = 0.52 x 10^{-5} cm^2. Thus, A_D = (0.5 + 1.5 + 1.5) x 10^{-3} cm^2 = 3.5 x 10^{-5} cm^2. The area remaining for interconnect is 5 x 10^{-5} cm^2.

4.5 Power Dissipation

The maximum power dissipated by a transmitter is given by

$$P_T \approx P_{max}(\text{laser}) + P_{max}(\text{driver}) \tag{48}$$

The maximum power dissipated by the laser is

$$P_{max}(\text{laser}) = I_{max}(V_J + I_{max} \; R_s) \tag{49}$$

for a junction voltage of 1.5 V and a series resistance of 2Ω.

$$P_{max} = 7 \text{ mA } (1.5 \text{ V} + 0.015)$$

$$= 10.6 \text{ mW}$$

For the TELD driver, the maximum power dissipated

$$P_{TELD} = I_{max} V_t \tag{50}$$

$$= 7 \text{ mA} \times 5 \text{ V} = 35 \text{ mW}$$

For the FET driver, the maximum power dissipated is

$$P_{FET} = I_{max} V_D \tag{51}$$

$$= 7 \text{ mA} \times 2 \text{ V} = 14 \text{ mW}$$

For the TELD-FET driver, the maximum power dissipated is

$$P_{T-F} = I_{max}^{(TELD)} V_t + I_{max}^{(laser)} V_D + I_{max}^2 \text{ (TELD) } R_1 \tag{52}$$

$$= 75 \text{ mW} + 14 \text{ mW} + 10 \text{ mW}$$

$$P_{T-F} = 100 \text{ mW}$$

From these examples, the minimum power dissipation is derived with the FET driver transmitter. The power dissipation is 1/2 of that of the TELD driver and 1/4 that of the TELD-FET driver. The power dissipation scales approximately linearly with laser drive current in all three cases.

To assess the impact of the transmitter power dissipation on the total power, we consider two cases of LSI circuits in GaAs and compare the transmitter power dissipation to the total circuit dissipation. The two cases for consideration are an 8 x 8 multiplier (1000 gates) and an 8 bit microprocessor. The multiplier circuit has been successfully fabricated at

Rockwell. The microprocessor is an ongoing goal of Rockwell's research program. It is anticipated that such a chip will require 10^5 gates. The estimated number of high speed output ports for each of these chips, is shown in Table III below.

Table III

	No. of Gates	No. of Output Ports	Projected Transmitter Power	Projected Total Power
8 x 8 multiplier	1000	10	250 mW FET 500 mW TELD 1150 mW TELD - FET	450 mW 700 mW 1350 mW
Microprocessor	10,000	24 8 data 12 address 4 control	600 mW FET 1200 mW TELD 2760 mW TELD - FET	20.6 2 W 21.2 W 22.76 W

In Table III, we have used projected values for the gate power mW/gate dissipation of 200 μm/gate. At present, the power dissipation is of the order 0.5-1.0 mW/gate. For projected chips of VLSI complexity, there is no severe penalty placed on the chip, on the average, to use optical interconnct, in that the power dissipated in the optical transmitter is far less than that dissipated on the chip. On the other hand, for chips of LSI complexity, the output part count and total power dissipation caused by using optical interconnct do not seem to justify the use of optical interconnect unless fanout per port is large. In this case the low drive penalty paid for relatively large fanout is in the favor of optical interconnect.

A final consideration with regard to power dissipation is the junction temperature experienced by the laser owning to local power dissipation. The thermal resistance of a junction up (or topside mounted) laser is 82.9 K/W.[59] For 14 mW dissipated in the laser, it will experience only ≈ 1-2° K use in T. If a heat spreading thick gold layer is added to the top. the heating is substantially reduced.

5.0 RECEIVER DESIGN

Each receiver port of an IC interconnect will require a high speed, sensitive detector-preamplifier. The characteristics of these devices are discussed below.

5.1 Detector Design

A high speed detector for application to IC interconnect must have sufficient sensitivity and bandwidth to detect the optical pulse energy available at the receiver from the optical distribution network. An avalanche photodiode based on GaAsAs/GaAs is the best choice for this application. The internal gain of an APD leads to improved signal-to-noise ratio as it increases the signal level with respect to the thermal noise of the amplifier or output circuit. Increasing the gain of an APD also has the undesirable effects of increasing dark current and noise and reducing the speed of response. Thus, there is an optimum APD gain which maximizes signal-to-noise, which is consistent with signal bandwidth or data rate.

An important consideration for a high speed application is the capacitance of diode which along with the preamp input capacitance will determine the maximum input resistance possible for a given bandwidth. The detector capacitance is dependent upon the doping level and size of the detector. This in turn will determine the feasibility of using the various interconnect schemes in a particular application.

To accommodate the APD with other processing procedures, the maximum epitaxial layer thickness that can be used is ~ 4 μm. Thus, an integrated APD on a semi-insulating substrate would be of the design shown in Fig. 30. Based on computer analysis of device response including avalanche gain, we would expect the maximum frequency of operation of such a device to be as shown in Fig. 31.

An alternate APD approach that is compatible with a waveguide technology is shown in Fig.32 . The area and thus capacitance of this device can be kept very small because of the small absorption depth of the GaAs active

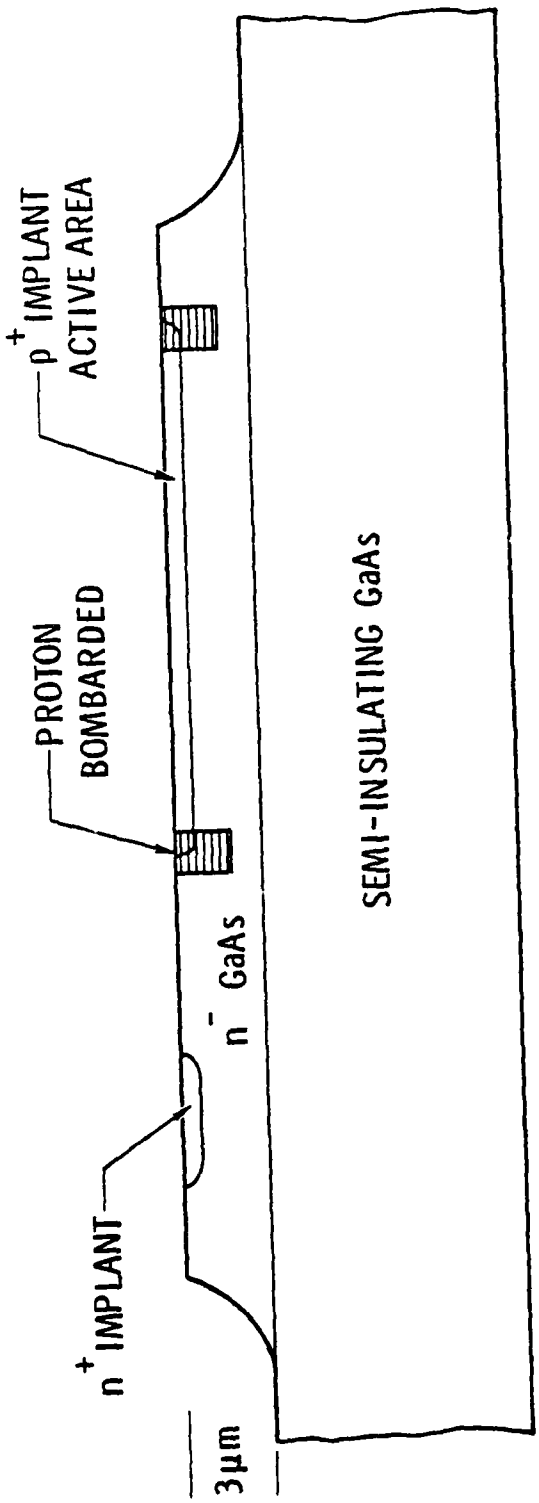
p+ IMPLANT
ACTIVE AREA
PROTON
BOMBARDED
SEMI-INSULATING GaAs
n- GaAs
n+ IMPLANT
3μm

Fig. 30

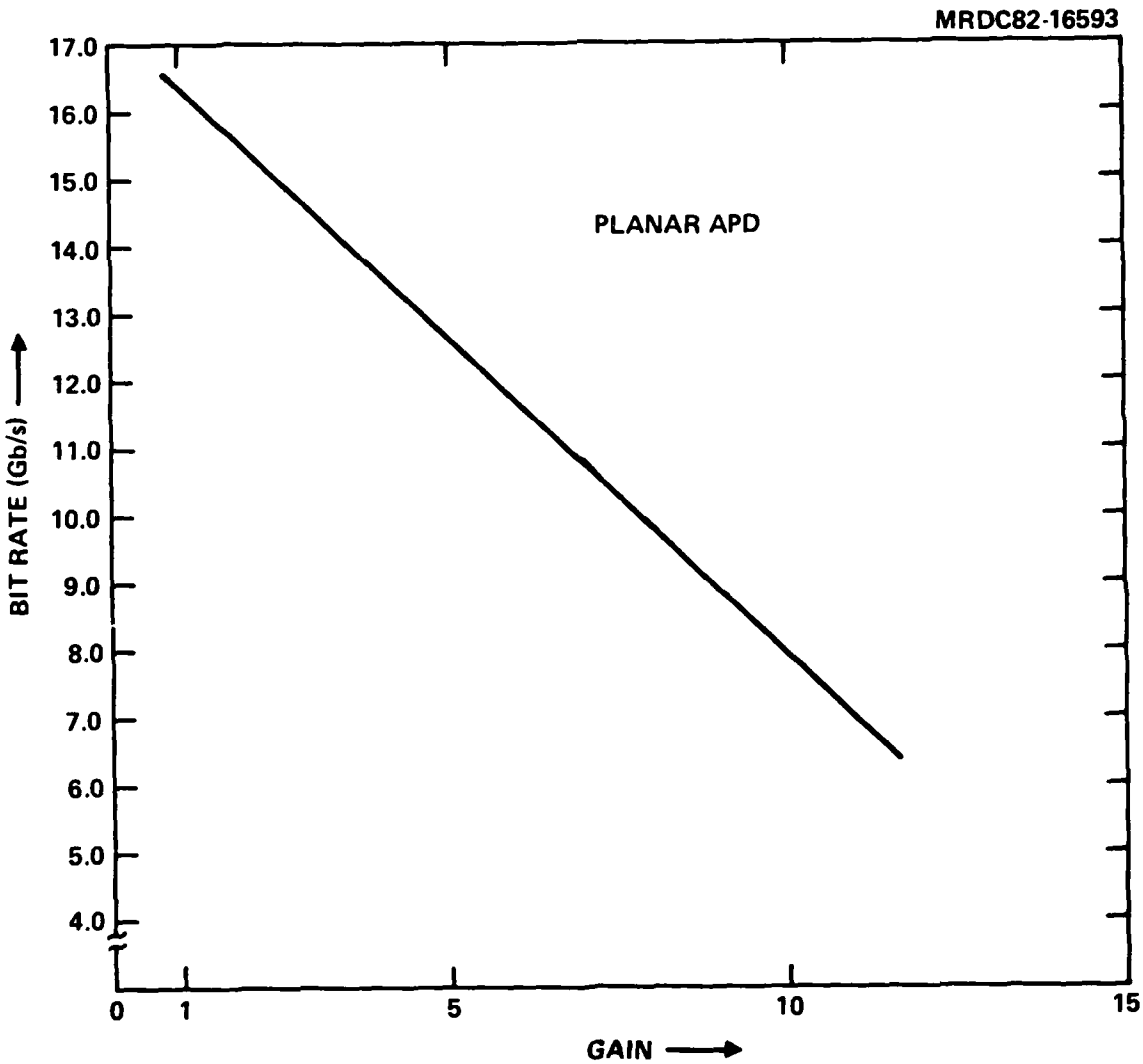
MRDC82-16593
PLANAR APD
BIT RATE (Gb/s)
17.0
16.0
15.0
14.0
13.0
12.0
11.0
10.0
9.0
8.0
7.0
6.0
5.0
4.0
0
1
5
10
15
GAIN

Fig. 31

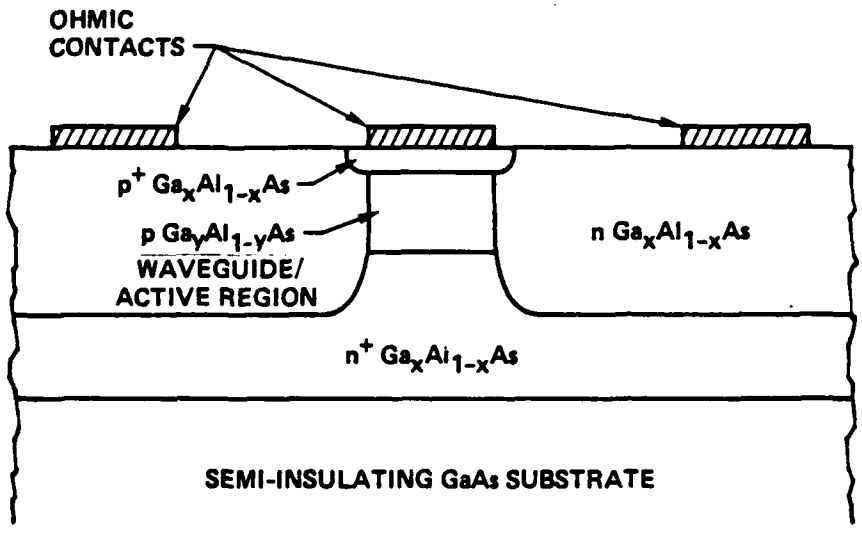
OHMIC
CONTACTS
p+ GaxAl1-xAs
p GayAl1-yAs
WAVEGUIDE/
ACTIVE REGION
n GaxAl1-xAs
n+ GaxAl1-xAs
SEMI-INSULATING GaAs SUBSTRATE

Fig. 32

region. However, the coupling of light from the optical distribution system into such a device will contribute large insertion losses. However, the device could be efficiently used in a system employing a planar waveguide.

Figure 12 shows the capacitance as a function of doping and carrier concentration for GaAs assuming infinitely thick GaAs. The restriction of the thickness of the GaAs to two to four μm limits the capacitance of any doping level to 6000 pf/cm^2 to 3000 pf/cm^2, respectively. As a result, the doping of the GaAs active region must be kept below 2×10^{16} cm^{-3}. The minimum size for a surface illuminated APD is of the order 50 μm x 50 μm to allow efficient coupling of radiation into the detector. Thus, the minimum capacitance would be of the order 0.075 pf. For a waveguide detector, the active area could be as small as 5 μm x 10 μm with a capacitance as low as 10^{-3} pf.

5.2 Amplifier Design

The design of a compact preamplifier for incorporation in the receiver port of an IC must allow high gain amplification at high speeds. The size constraints on such a preamplifier are similar to those on the transmitter. It is desirable to reduce the receiver port to as small a dimension as possible.

Bandwidth

The bandwidth of the preamplifier is determined by the $R_L C_T$ time constant of the input stage. C_T is the total input capacitance including the detector depletion capacitance, C_D the gate capacitance of the input FET, C_g and the stray capacitance C_S for a monolithically integrated receiver $C_S \ll C_D$ and $C_g \ll C_D$. Thus,

$$B = \frac{1}{2\pi C_D R_L} \tag{53}$$

For a 5 GHz bandwidth $R_L \lesssim 400\ \Omega$, if $C_D = 0.075$ pf.

Noise

The minimum average square of the noise current for an FET front end if load resistor $R_L \to \infty$ is determined by the FET parameters and the total capacitance.(60)

$$\langle i^2 \rangle_{min} = 4kT\Gamma \frac{(2\pi C_D)^2}{g_m} B^3 I_3 \tag{54}$$

where Γ and I_3 are numerical factors determined by materials parameters and spectral properties of the pulse shape and transfer function, respectively, g_m is the transconductance. The numerical value of $\langle i^2 \rangle_{min}$ for typical GaAs FET parameters is given by

$$\langle i^2 \rangle \approx 1.1 \times 10^{-17} B^3 A^2 \tag{55}$$

where B is in Gb/s.

The noise current contributed by the load resistor is given by

$$\langle i^2 \rangle_{R_L} = \frac{4kT}{R_L} I_3 B \tag{56}$$
$$\approx \frac{1.6 \times 10^{-11}}{R_L} B A^2$$

where B is in Gb/s.

For R_L to achieve a bandwidth of 5 GHz, the noise current contributed by the load resistor dominates the noise of the front end.

Amplification

The required amplification of the preamp to result in voltage outputs suitable for typical voltage swings of 0.5 V can be estimated by considering Fig. 18, where we show the minimum received power vs frequency for an APD. Note that for system interconnected with a guided wave, the minimum received power is determined by the number, N, of connected terminals or chips (fanout).

For a large fanout, N = 100, the maximum received power is - 26 dBm. A received power of - 26 dBm results in 2.5 μA of collected current. For a gain of 10 in the APD, this results in a signal of 6.3 mV across a 250 Ω load resistor. To achieve logic levels of 0.5 V will require a voltage gain of ≈ 100. This can be obtained by using a three stage amplifier with 0.5 μm gate length technology FET's.

Size

The dominant factors in the size of the receiver are the detector and output transistor. The detector must be 50 μm x 50 μm in geometry for surface coupled applications. For edge or waveguide coupled applications, the waveguide detector could in principle be much smaller. The output transistor of the preamplifier must drive a 50 load at 10 mA to achieve 0.5 V logic levels. This requires a 10 to 20 mA saturation current. A 50 μm wide transistor is required to produce this saturation current. As a result, the output transistor is ≈ 10 μm x 50 μm in size. From these constraints, the average size of the receiver can be kept well below 10^{-4} cm^2. Power dissipation is controlled by the output transistor. We estimate that

$$P_T \approx 0.5 \times 10 \text{ mA} \times 2 \text{ V} = 10 \text{ mW}.$$

6.0 TECHNOLOGY TRADEOFFS

In order to properly assess various specific schemes to optically interconnecting IC's, it is necessary to consider the various technology tradeoffs in the elements of an optical interconnected system. The elements under consideration are:

(1) Optical distribution system
(2) Transmitter and receiver design
(3) Transmitter and detector fabrication technology.

Each of the tradeoffs is considered in detail below.

6.1 Optical Distribution System: Guided Wave vs Broadcast Interconnect

This represents the most critical tradeoff as it will determine the course in many of the others. Since it is anticipated that GaAs IC's will be operating in the four to five Gb/s range, the sensitivity of optimized receivers is limited. As a result the optical losses in transmission of information from one terminal to another is limited to - >27dB for a signal to noise ratio of 100 (BER < 1E - 10). Broadcast interconnection of devices on a 10 cm x 10 cm broad would require the use of large area detectors (Area = 0.1 cm^2). This is excessively large for inclusion on a GaAs IC. On the other hand, if the interconnection were to occur over smaller areas; i.e., 1 cm x 1 cm, detectors with 10^{-3} cm^2 area would be satisfactory and practical. Guided wave interconnect allows a large fanout of the data owing to the selective nature of the transmission. The information is divided into N parts, where N is the number of ports to be interconnected. Even for fanouts as large 100, a guided wave interconnect system appears to easily meet the noise margin. This is true for interconnect schemes based on optical fibers where no loss occurs during transmission. In addition to greater losses, the broadcast approach results in greater propagation delay. The minimum distance travelled by a photon in going from one transmitter port to another is 20 cm. The delay caused by the traversal of this distance is T_d = D/c or 2 ns

for a nearest neighbor. The skew of the delay to chips at various distances from the transmitter is $\Delta T_d = (X_{max} - D)/c$.

6.2 Optical Distribution System: Fibers vs Planar Waveguides

To accommodate large fanouts and complicated interconnects, optical fibers are the choice in this comparison. Fibers are essentially lossless and thus contribute no loss other than coupling and distribution losses. Owing to their flexibility, fibers also can accommodate complicated topologies more readily than planar waveguides.

	Coupling Losses	Distribution Losses
Fibers	3 dB	1/N
Waveguides	3 db	$1/N + \alpha D$

Waveguides, on the other hand, are quite lossy $\alpha > 0.6$ dB/cm. For large fanouts or long distances the losses in waveguide system become too large. However, for point-to-point interconnect over short distances, waveguides interconnect would be totally suitable.

6.3 Optical Distribution System: Edge Coupling vs Perpendicular Coupling

The particular direction of coupling is irrelevant for a guided wave distribution system based on optical fibers. The problem becomes one of alignment of the fibers to the sources and detectors. For planar waveguides, edge coupling is preferred to simplify the alignment and waveguide fabrication. However, perpendicular coupling could be accommodated by the use of grating couplers in the waveguides. Broadcast interconnect is most simply accomplished with perpendicular coupling of the light. It should be noted that the use of perpendicular coupling requires the use of grating fabrication in the laser.

6.4 Transmitter Design: Planar vs Epitaxial Laser Designs

A major consideration in the use of optical interconnect is drive power necessary to support; this form of interconnect. As was pointed out in a previous section, the dissipated power in a transmitter port scales linearly with the drive current of the laser. As a result, low threshold and high differential quantum efficiency are required for the laser design. In addition, the structure must be easily integrable with the circuitry.

The epitaxial buried heterostructure laser is the only design that appears to couple low enough threshold and high efficiency. As a result, it appears the most desirable device structure for an IC transmitter. However, the integration to this structure with the GaAs ion implantation technology predominant for IC's is difficult at the present time. Although the structure can in principle be grown into grooves in the top surface similar to Rockwell's present approach, the processing is complicated and will most likely be low yield.

To facilitate the use of advanced epitaxial laser designs in transmitter ports, development in two areas is necessary: (1) Localized epitaxial growth (see Fig. 27), and (2) Backside wafer processing (see Fig. 28). Localized epitaxy facilitates the fabrication of buried heterostructures and permits the fabrication of the different materials required for lasers and detectors in one growth run. The latter point is of importance to minimize the cost. Backside processing relaxes the constraints on device size, permits the fabrication for redundant devices, improves the possibility for efficient heat sinking, and reduces the interaction between optical and electrical devices. Low resistance electrical vias must be developed before this becomes a reality.

6.5 Transmitter Design: Etched Mirror Lasers vs Distributed Feedback Lasers

DFB or DBR lasers require the routine fabrication of efficient first order gratings. The period of the corrugations is approximately 1750 A. The high efficiency requirement implies that the grating depth must be > 1000 A. This is a difficult task that requires a great deal of development. Second

order gratings with periods 2450 Å and depth 1500 Å are required for perpendicular coupling. Grating based lasers provide superior frequency selectivity and stability, but these are not expected to be important for IC interconnect. Etched mirror lasers on, the other hand, do not require the holographic or E-beam lithography required for grating fabrication. This greatly simplifies the fabrication and will lower the cost of the circuit fabrication. Based on the ease of fabrication, adequate frequency selectivity, and lower cost, etched mirror lasers appear to be the best choice. However, should perpendicular coupling of the light be required for a particular interconnect scheme, grating lasers will be required.

6.6 Receiver Design: Avalanche vs PIN Photodiodes

The analysis of Section 2.0 clearly showed that to accommodate a five Gb/s data rate in a system with large losses, an avalanche photodiode is required. The optimum gain for operation at five Gb/s and BER of 1E-10 can be determined from the plot of Fig. 33. Clearly the minimum required power occurs at a gain of eight.

For a system with small fanout and small losses in the interconnect network, however, a gain of one could be accommodated. The specific system layout and interconnect will determine the gain for the detectors.

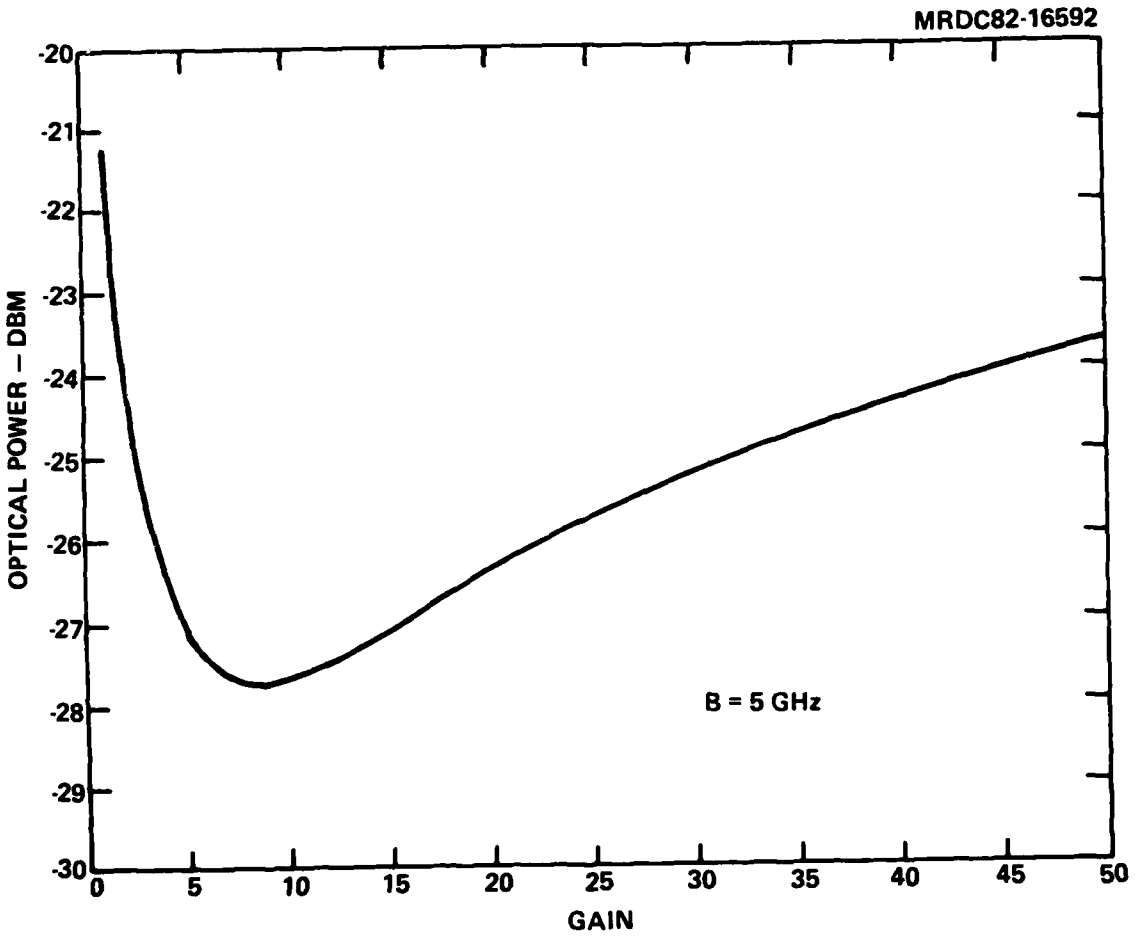
MRDC82-16592
OPTICAL POWER – DBM
-20
-21
-22
-23
-24
-25
-26
-27
-28
-29
-30
0
5
10
15
20
25
30
35
40
45
50
GAIN
B = 5 GHz

Fig. 33

7.0 INTERCONNECT DESIGNS

From the results of the previous sections, it is clear that no one interconnect scheme applies to all interconnect problems. However, each system design must have the choice of utilizing the appropriate interconnect schemes. In this section, we show examples of three optical interconnect schemes that are viable approaches for certain systems applications based on the analysis of the previous sections. They bear close similarity to local network designs commonly in use to interconnct computers and peripherals.

7.1 Local Broadcast (LB) Interconnect

Local broadcast interconncect is an approach for the interconnection of terminals on a chip with one another. It can be used as anelement in the design of GaAs integrated circuits to increase layout flexibility of complex GaAs subsystem chips. The general idea is embodied in the illustration of Fig. 13. Here we show a GaAs IC with distributed transmitter and receiver ports on the surface of the chip. Interconnection of various subsystem parts is accomplished by broadcasting these data in free space to all the receiver ports on the chip. The analysis of Section 3.5 indicated that this scheme is practical for areas up to 1 cm x 1 cm at four GHz. The major advantage of this interconnect approach is simplicity. No alignment of fibers or guides is necessary. The interconnect is accomplished by the packaging of the circuit. The major disadvantage of the approach is the inevitable need for complex transmitter design -- particularly the laser. LB interconnect can only be effectively achieved if the lasers emit their light perpendicular to the surface in which they lie. As discussion in earlier sections has pointed out, this is accomplished with the use of distributed feedback gratings. In principle, gratings can be fabricated to perform this function but only with great difficulty at the present time. The neccessary technology for the implementation of LB interconnect is listed below.

TRANSMITTER:
BH lasers with second order coupling gratings
Etched mirrors
FET Drivers
Backside processing

RECEIVER:
Surface Detector
Three stage preamp
Backside processing

The losses in this approach are primarily the distribution losses. If the area of the detector is 10^{-4} cm^2, the losses to interconnect ports on a 1 cm x 1 cm surface area are -40 dB. To achieve the required sensitivity, the laser must emit 10-20 mW of power. Larger area detectors can be used with an increase in the average received power only if the backside processing approach is used.

7.2 Direct/Relay Interconnect

The most direct method of interconnecting IC's on a system board is to interconnect the various terminals directly as would be done in an electrically interconnected system. In principle, this can be done by the use of optical fibers or planar waveguides. However, this approach quickly becomes inadequate when several terminals must be interconnected (i.e., large fanout). To accommodate this possibility, we consider the system design illustrated in Fig. 34. In this system design local subsystem interconnection is accomplished by direct point-to-point terminal interconnect. This is usually feasible for major subsystem chips and their support chips. Interconnection of subsystem segments is accomplished by optical relay chips. These chips decode the addresses of the receiver subsystem and either relay these data to the next subsystem mode or transfer it to the appropriate subsystem that is serves. Broadcast interconnect to the various subsystems can be accommodated by the

AD-A112 239 ROCKWELL INTERNATIONAL THOUSAND OAKS CA MICROELECTR--ETC F/G 20/6
OPTICAL COMMUNICATION FOR INTEGRATED CIRCUITS.(U)
MAR 82 P D DAPKUS N00014-80-C-0501
UNCLASSIFIED MRDC41072.1FR NL

END
DATE FILMED
4 82
DTIC

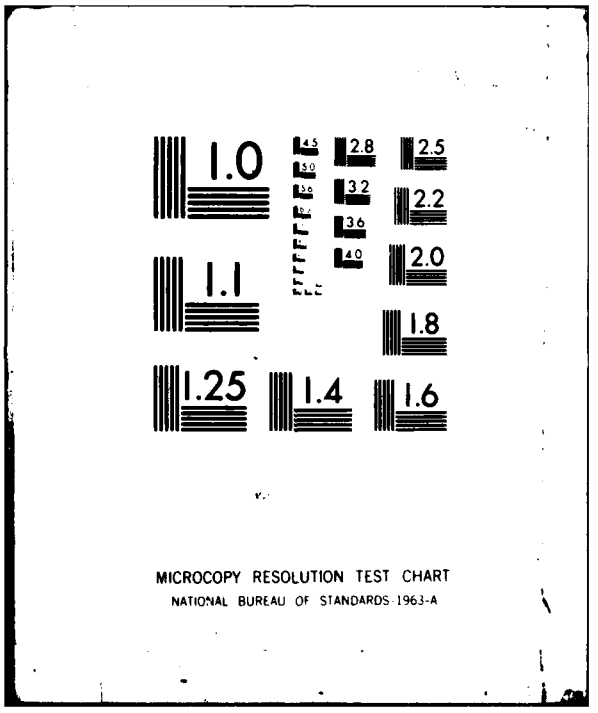
1.0
1.1
1.25
1.4
1.6
1.8
2.0
2.2
2.5
2.8
3.2
3.6
4.0
MICROCOPY RESOLUTION TEST CHART
NATIONAL BUREAU OF STANDARDS-1963-A

MRDC82-16591

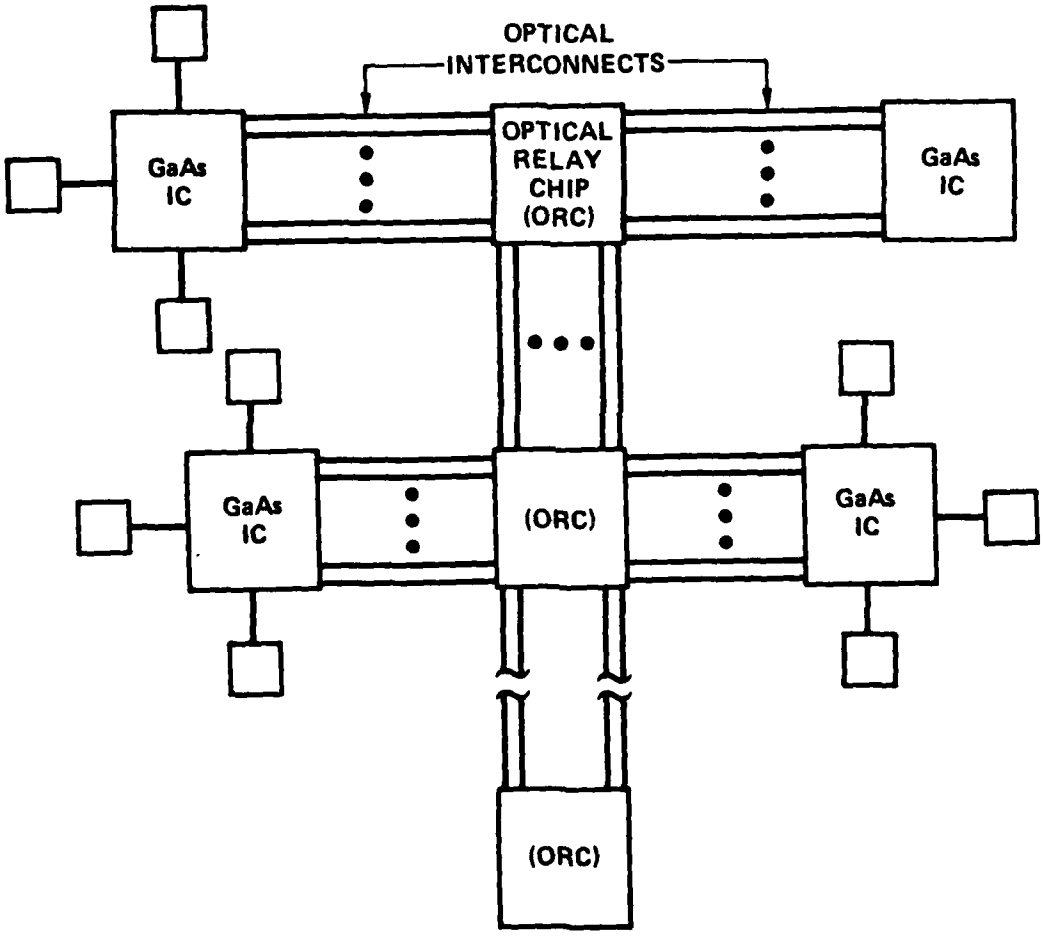

Fig. 34

appropriate address. There are important advantages to direct/relay (D/R) interconnect that should be illucidated. The fanout to various terminals is never greater than one. As a result, significant losses in the coupling of the light to the waveguide and within the waveguide are possible without substantially affecting the system performance. Alternatively lower output powers from the lasers can be utilized which may reduce the drive current substantially. Owing to the reduced importance of high coupling efficiency and low losses, this scheme can most likely be achieved with relatively low cost alignment schemes and low cost planar waveguides. Since the separation between various chips is envisioned to be less than 1 cm, time delay between chips will be significantly less than one clock cycle, and protocol can easily be arranged to avoid data collisions. For simple systems with one controller, this is not a particular problem since communications are determined by the controller. The major potential disadvantages of D/R interconnect are the limited fanout and delays between nodes. Typical relay times for a given node may be as long as 1 ns which limits the effective data transfer rate between subsystems.

The technology requirements to implement D/R interconnect are specified below.

TRANSMITTER:
Etched mirror BH laser
Edged coupled laser
FET driver
Backside Processing

RECEIVER:
Waveguide Detector
One to Two Stage Preamp
Backside Processing

OPTICAL DISTRIBUTION SYSTEM:
Guided Wave System
Planar Waveguides

To assess the losses in such a system, we need consider only the losses in one leg of the system, since the data always regenerated.

Laser to waveguide coupling loss	-- 3.0 dB
Waveguide losses	-- 0.6 dB
Waveguide to detector coupling loss	-- 3.0 dB

The total loss per leg is 6.6 dB. This is considerably lower than the allowed losses calculated in Section 3.5.

7.3 Fiber Star Interconnect

Another guided wave interconnect approach is the fiber star (FS) interconnect approach. In this approach, fanout and selective interconnect are achieved by the fiber network utilized to interconnect the ports. Figure 35 shows an illustration of a FS interconnected system. The major advantages of such a system are the low coupling losses, immediate data transmission, and the system flexibilty. The major disadvantage is the complexity of the hybrid interconnection. However, with the use of precisely machined alignment fixtures and automated assembly, even this can be overcome. The task is certainly no more difficult than the wiring done on present computer boards.

The necessary technology development to implement this approach is listed below.

TRANSMITTER:
BH laser with distributed feedback coupling grating
Etched mirrors

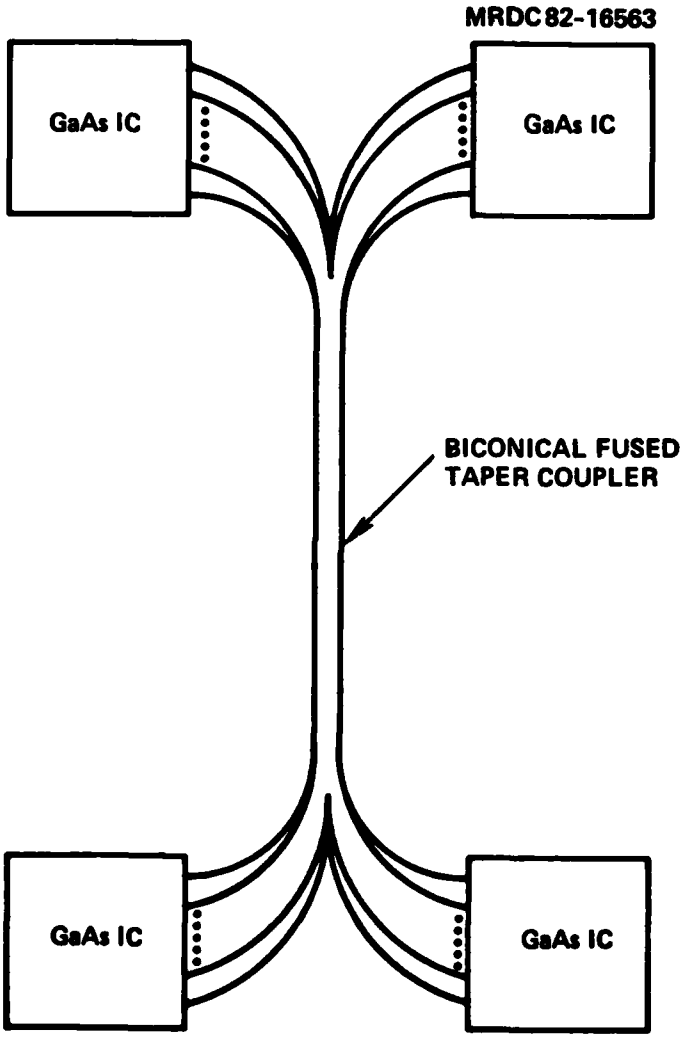
MRDC82-16563
GaAs IC
GaAs IC
BICONICAL FUSED
TAPER COUPLER
GaAs IC
GaAs IC

Fig. 35

RECEIVER:
Surface detector
Two or three stage preamp

OPTICAL DISTRIBUTION SYSTEM
Fiber star couplers

The losses in this approach are summarized below

Laser to optical fiber coupling	-- 3.0 dB
Distribution losses	-- 10.0 dB
Fiber to detector losses	1.0 dB

Thus, the total signal available at the receiver if the laser emits 1.0 mW of power is -14 dBm. This is well above the minimum acceptable power and leaves margin for considerable other losses in the system.

8.0 CONCLUSIONS AND RECOMMENDATIONS

The analysis presented in this report has focussed on the feasibility of optically interconnecting very high speed GaAs integrated circuits. To determine if optical interconnect is feasible, it has examined each element of such a system, determined the optimum parameters for use in an optically interconnected system, and predicted the performance of the element in the system use. As a result of this analysis, a number of general and specific conclusions and recommendations are presented in this section.

8.1 Conclusions

The major conclusions to be reached from this study are:

1. Optical interconnect is possible and sensible for very high speed integrated circuits provided that continued development of certain key technologies is continued.
2. Optical interconnect requires the availability of on-chip optical devices to be feasible and practical.
3. There is no single optical interconnect approach suitable for all applications. Rather, each system application will require separate consideration and design. As a result the generic technology development must be performed to provide the system designer with options for interconnect.
4. Optical interconnection of circuits on a circuit board must utilize guided optical waves, so that sufficient noise immunity is achieved.
5. On-chip interconnect is possible with free space broadcast interconnect.
6. Input and output terminals with dimension comparable to present day bonding pads are feasible.
7. Power dissipation for optical device elements can be made a small fraction of total chip power dissipation.
8. All high speed data input and output can be performed by optical means.

9. Significant technology development is required before optical interconnect can be routinely used in system interconnect.

8.2 Recommendations

The recommendations that result from this study are concerned with the technology development that must be performed to make optical interconnect a reality.

1. The continued exploration of the technology for integrating the optical devices with electronic devices is needed. Focus should be given to the development of backside processing techniques to increase the flexibility of the integrated optoelectronics technology.

2. The development of very low threshold lasers based on the buried heterostructure design must be pursued. The goal of this development is technology for the fabrication of lasers with less than 5 mA threshold current and very high quantum efficiency operation.

3. The development of distrubuted feedback grating technology to allow the fabrication of efficient first and second order gratings must be undertaken.

4. Etched mirror lasers for use in optical interconnect must be developed.

5. Further development of high speed, high efficiency photodiodes is required.

6. Further development of low loss planar optical waveguides is required.

7. Advanced fabrication techniques for the formation of fiber couplers are required.

A plan to utilize optical interconnect in a GaAs IC system should be based around a specific system under development. The most practical system under near term development that will require an optical interconnect is a GaAs microprocessor system. The development of this chip set including a CPU,

cache memory and bulk memory is being pursued at Rockwell. It is anticipated that by 1987 this chip set will have been demonstrated. To incorporate an optical interconnect onto such a system will require immediate attention to generic technology development. The specific development pertinent to the microprocessor can be addressed within the microprocessor program. The program for technology development should address generic development needs until the architecture of the system is well defined. Decisions can then be made as to the specific configuration to be used. This plan assumes an ongoing program to develop a high capacity fiber optic bus and uses the technology developed in that program. A decision point is planned after three years to assess the practicality of optical interconnect vis a vis other technologies.

Three general areas require development:

1. Integrated lasers with ultra low threshold
2. Integrated detectors
3. Optical distribution networks

Lasers

The goal of this development area is to develop a laser technology suitable for integration with complex GaAs IC's and that also operate with very low threshold currents (< 5 ma). The choice of a buried heterostructure design makes the achievement of back-side processing more desirable. This technology should be developed to assess the merits and advantages vis a vis conventional processing. The incorporation of grating into laser design will require that significant development be given this area. Some of this will be done in conjunction with the fiber bus development, but additional work particularly in the area of second order grating couplers should be done here.

Detectors

The major area development needed for IC interconnect is the development of large-area, low-capacitance detectors for possible use in broadcast interconnect system.

Optical Distribution Network

Various network options will be explored to determine losses and fabrication procedures. Fiber and planar waveguide networks must be developed for this application as well as the means for hybrid coupling these networks to arrays of lasers and detectors.

Rockwell International

MRDC41072.1FR

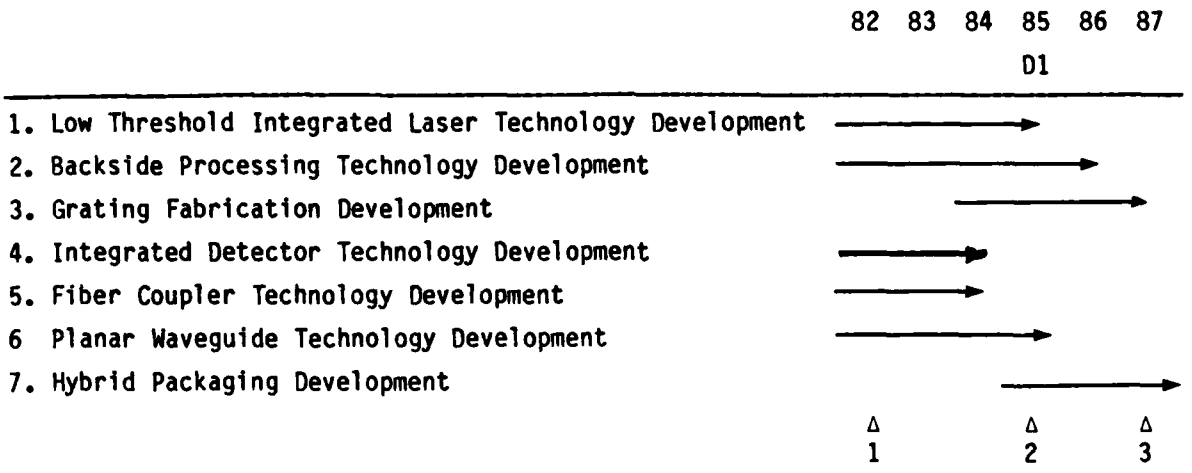

D-1 Decision point - Assess practicality of optical interconnect.

Δ 1. Demonstration of integrated transmitter and receiver.

Δ 2. Demonstration of microprocessor chip.

Δ 3. Demonstration of optically interconnected microprocessor system.

9.0 REFERENCES

1. R. D. Dupuis, J. Cryst. Growth 55, 213 (1981).

2. N. Chinone, H. Nakashima, I. Ikushima, and R. Ito, Appl. Opt. 17, 311 (1978).

3. T. Korayashi, H. Kawaguchi, and Y. Furukawa, Jpn J. Appl. Phys. 16, 601 (1977).

4. R. D. Burnham, D. R. Scifres, and W. Streifer, Appl. Phys. Lett. 40, 118 (1982).

5. H. Yonezu, et al, Jpn. J. Appl. Phys. 16, 209 (1977).

6. E. Bourkoff, SPIE Integrated Optics 269, 25 (1981).

7. C. S. Hong, J. J. Coleman, P. D. Dapkus, and Y. Z. Liu, Appl. Phys. Lett. 40, 208 (1982).

8. H. Kumabe, T. Tanaka, H. Namizaki, M. Ishii, and W. Susaki, Appl. Phys. Lett. 33, 38 (1978).

9. M. Nagano and K. Kasahara, IEEE QE-13, 532 (1977).

10. R. Tell and S. T. Eng, Electron. Lett. 16, 497 (1980).

11. T. Tsukada, J. Appl. Phys. 45, 4899 (1974).

12. R. D. Burnham and D. R. Scifres, Appl. Phys. Lett. 27, 510 (1975).

13. T. Kobayashi and S. Takahashi, Jpn. J. Appl. Phys. 15, 2025 (1976).

14. W. T. Tsang and R. A. Logan, IEEE QE-15, 451 (1979).

15. N. Chinone, K. Saito, R. Ito, K. Aiki, and N. Shige, Appl. Phys. Lett. 35, 513 (1979).

16. J. Katz, S. Margalit, D. Wilt, P. C. Chen, and A. Yariv, Appl. Phys. Lett. 37, 987 (1980).

17. Y. Mori, O. Matsuda, and N. Watanabe, J. Appl. Phys. 5429 (1981).

18. T. L. Paoli and J. E. Ripper, IEEE Proc. 58, 1457 (1970).

19. N. Chinone, K. Aiki, M. Nakamura, and R. Ito, IEEE QE-14, 625 (1978).

20. G. Arnold and P. Russer, Appl. Phys. 14, 255 (1977).

21. G. Arnold and K. Petermann, Optical Quantum Electron. 10, 311 (1978).

22. P. Torphammar, R. Tell, H. Eklund, and A. R. Johnston, IEEE QE-15, 1271 (1979).

23. K. Y. Lau and A. Yariv, Opt. Commun. 35, 337 (1980).

24. J. Au Yeung and A. R. Johnston, SPIE Integrated Optics 269, 84 (1981).

25. D. Wilt, K. Y. Lau, and A. Yariv, J. Appl. Phys. 52, 4970 (1981).

26. D. Fekete, W. Streifer, D. R. Scifres, and R. D. Burnham, Appl. Phys. Lett. 37, 975 (1980).

27. H. Kressel and J. K. Butler, *Semiconductor Lasers and Heterojunction LED's* (Academic Press, New York, 1977), p. 101.

28. H. D. Law, K. Nakano, and L. R. Tomasetta, IEEE QE-15, 549 (1979).

29. H. D. Law, K. Nakano, and L. R. Tomasetta, Appl. Phys. Lett. 35, 180 (1979).

30. I. Ury, S. Margalit, M. Yust, and A. Yariv, Appl. Phys. Lett. 34, 430 (1978).

31. J. Katz, et al, Appl. Phys. Lett. 37, 211 (1980).

32. C. P. Lee, S. Margalit, I. Ury, and A. Yariv, Appl. Phys. Lett. 32, 806 (1978).

33. T. Fuzukawa, M. Nakamura, M. Hirao, T. Kuroda, and J. Umeda, presented at Topical Meeting on Integrated and Guided Wave Optics (1980), unpublished.

34. M. Yust, et al, Appl. Phys. Lett. 35, 795 (1979).

35. T. Ozeki and B. S. Kawasaki, Electron. Lett. 12, 151 (1976).

36. E. G. Rawson and A. B. Nafarrate, Electron. Lett. 14, 274 (1978).

37. F. Szarka, A. Lightstone, J. Lit, and R. Hughes, Fiber Integrated Optics 3, 285 (1980).

38. J. T. Boyd, Appl. Phys. Lett. 37, 512 (1980).

39. S. Dutta, H. E. Jackson, J. T. Boyd, F. S. Hickernell, and R. L. Davis, Appl. Phys. Lett. 39, 206 (1981).

40. W. B. Joyce, R. A. Bachrach, R. W. Dixon, and D. A. Sealer, J. Appl. Phys. 45, 2229 (1974).

41. G. E. Stillman and C. M. Wolfe, *Semiconductors and Semimetals*, R. K. Willardson and A. Beer, ed., Vol. 12 (Academic Press, New York, 1966), p. 291.

42. J. L. Merz and R. A. Logan, Appl. Phys. Lett. 30, 530 (1977).

43. P. D. Wright and R. J. Nelson, IEEE EDL-1, 242 (1980).

44. S. Adachi and H. Kawaguchi, J. Appl. Phys. 52, 3176 (1981).

45. L. A. Coldren, K. Iga, B. I. Miller, and J. A. Rentschler, Appl. Phys. Lett. 37, 681 (1980).

46. A. Yariv, IEEE QE-9, 919 (1973).

47. A. Yariv and H. W. Yen, Opt. Commun. 10, 120 (1974).

48. M. Nakamura and A. Yariv, Opt. Commun. 11, 18 (1974).

49. M. Nakamura, et al, IEEE QE-11, 436 (1975).

50. H. C. Casey, Jr., S. Somekh, and M. Llegems, Appl. Phys. Lett. 27, 142 (1975).

51. K. Aiki, et al, Appl. Phys. Lett. 27, 145 (1975).

52. M. Nakamura, K. Aiki, J. Umeda, and A. Yariv, Appl. Phys. Lett. 27, 403 (1975).

53. H. W. Yen, W. Ng., I. Samid, and A. Yariv, Opt. Commun. 17, 213 (1976).

54. R. D. Burnham, D. R. Scifres, and W. Streifer, Appl. Phys. Lett. 29, 287 (1976).

55. W. Ng, H. W. Yen, A. Katzir, I. Samid, and A. Yariv, Appl. Phys. Lett. 29, 684 (1976).

56. W. Ng and A. Yariv, Appl. Phys. Lett. 31, 613 (1977).

57. W. W. Ng, C. S. Hong, and A. Yariv, IEEE T-ED-25, 1193 (1978).

58. T. R. Anthony, J. Appl. Phys. 52, 5340 (1981).

59. W. B. Joyce and R. W. Dixon, J. Appl. Phys. 46, 855 (1975).

60. R. G. Smith and S. D. Personich, *Topics in Applied Physics: Semiconductor Devices for Optical Communication*, H. Kressel, ed. (Springer Verlag, Berlin, 1980), pp. 89-159.

END

DATE
FILMED
4-82

DTIC